Observable Hyperfine Effects in Muon Capture by Complex Nuclei*†

ROLAND WINSTON
The Enrico Fermi Institute for Nuclear Studies, The University of Chicago, Chicago, Illinois
(Received 27 August 1962)

The capture rates, $\Lambda_{\pm}^{\text{cap}}$, of the two hyperfine states $F_{\pm}$ of the $(p\mu)$ atom are, in general, expected to be different (spin dependence of muon capture). This difference depends quantitatively on the details of the interaction Hamiltonian, being maximum for an F−GT (i.e., $V-A$ type) interaction. An experimental comparison for the $(p\mu)$ system appears at present difficult, but related spin-dependence effects will be exhibited by bound protons, i.e., complex nuclei. Observable hyperfine (hf) effects of this kind form the object of this paper; their theory is summarized in Sec. II. The character of such effects is dominated by the rate R at which the upper hf state can be converted into the true ground state (through an $M1$ Auger process). Section III contains a detailed calculation of R for all cases of practical interest, while a variety of possible experiments are discussed in Sec. IV. The considerations of this section show that F^{19} constitutes the ideal target, leading to the largest and most readily analyzable effects. We performed three experiments with this target, viz., measured (1) the time distribution of the neutral capture products, (2) the asymmetry of the decay electrons, and (3) the time distribution of the latter; these measurements are described and analyzed in Secs. V through VII. We conclude (Sec. VIII) on the basis of measurements (1) and (3) that the interaction is definitely of the F−GT (as opposed to F+GT) type, assuming that both F and GT interactions are present. Invoking independent observations on muon capture by complex nuclei, this assumption becomes redundant, and we may conclude that the universal Fermi interaction ("$V-xA$") is implied by our results. This conclusion is in agreement with recent results on muon capture in liquid hydrogen. The conversion rate observed in experiments (1) and (3) (6.1 ± 0.7 μsec^{-1}) agrees with our prediction ($R=5.8$ μsec^{-1}), which is qualitatively confirmed by experiment (2).

I. INTRODUCTION

IDEALLY, the study of muon capture would consist in determining experimentally as many (or more) observable parameters of the fundamental reaction

$$p+\mu^-(\text{atom})\rightarrow n+\nu \qquad (1)$$

as the number of independent couplings entering into the interaction Hamiltonian responsible for (1). In practice, a more modest approach is taken: One makes the assumption of a universal Fermi interaction (UFI), i.e., that the Hamiltonian in question is essentially the same as that established for e capture (the well known "$V-xA$" interaction), and checks the *consistency* of experimentally observed parameters with the predictions of the UFI assumptions. The nonrelativistic UFI Hamiltonian for muon capture[1] contains three parameters (G_V, G_A, and G_P), so that at least three experimental parameters of (1) must be determined; the actual observation of muon capture in *liquid hydrogen*—not in mesonic hydrogen atoms—has only very recently been achieved,[2–4] and has yielded only one observable parameter, the capture rate (which was found to be consistent with UFI). Under these circumstances, even greater modesty of aims imposes itself, and one should attempt to use experiments on muon capture by *complex nuclei*—though admittedly less direct than those on the fundamental reaction itself—to verify the presumed universality.

The information gained to date from capture experiments with complex nuclei can be summarized as follows:

(a) The Gamow-Teller coupling constant in μ capture, G_G (presumably G_A), has essentially the UFI predicted absolute magnitude; this follows from a comparison of the rates $C^{12}+\mu^-\rightarrow B^{12}$ (g.s.)$+\nu$ and $B^{12}\rightarrow C^{12}+e^-+\bar{\nu}$ (Godfrey-Tiomno cycle), and, more indirectly, from the observed branching ratio

$$(\pi^+\rightarrow e^++\nu)/(\pi^+\rightarrow\mu^++\nu).$$

(b) The spin-averaged "hydrogen" capture rate, $\bar{\Lambda}^{\text{cap}}(1,1)$, extracted from a fit of the *total* capture rates of many complex nuclei to Primakoff's closure formula[1] can be used to put a lower limit on the absolute magnitude of the Fermi coupling constant G_F (presumably G_V) in muon capture. The observed $\bar{\Lambda}^{\text{cap}}(1,1)$ is in excellent accord with UFI, and rules out the *absence* of a Fermi coupling.[5]

(c) The magnitude of the neutron asymmetry parameter in muon capture[6–8] requires the emission of a left-handed neutrino[9] and the presence of an induced pseudoscalar interaction of the strength and phase

* Research supported by a joint program of the Office of Naval Research and the U. S. Atomic Energy Commission.
† Based on a thesis submitted to the Faculty of the Department of Physics, the University of Chicago, in partial fulfillment of the requirements for the Ph.D. degree.
[1] H. Primakoff, Rev. Mod. Phys. 31, 802 (1959).
[2] R. H. Hildebrand, Phys. Rev. Letters 8, 34 (1962).
[3] E. Bleser, L. M. Lederman, J. Rosen, J. Rothberg, and E. Zavattini, Phys. Rev. Letters 8, 288 (1962).
[4] CERN—Bologna Collaboration (private communication), from C. Rubbia to V. L. Telegdi.
[5] V. L. Telegdi, Phys. Rev. Letters 8, 288 (1962).
[6] A. Astbury, I. M. Blair, M. Hussain, M. A. R. Kemp, H. Muirhead, and R. G. P. Voss, Phys. Rev. Letters 3, 476 (1959).
[7] V. L. Telegdi, in *Proceedings of the 1960 Annual International Conference on High-Energy Physics at Rochester*, edited by E. C. G. Sudarshan, J. H. Tinlot, and A. C. Melissinos (Interscience Publishers, Inc., New York, 1960), p. 713.
[8] A. Astbury, J. H. Bartley, I. M. Blair, M. A. R. Kemp, H. Muirhead, and T. Woodhead (to be published).
[9] This assumes that the captured μ^- is right handed; this was recently proved by Møller scattering (CERN) and by Mott scattering (Columbia). Cf. reference 7.

currently postulated for UFI, i.e., $G_A/G_P \approx 2.2$.[1] [Note that this information is actually needed to draw conclusion (a) above.]

Note that one cannot from (a) and (b) draw even the qualitative conclusion that UFI holds, because these are statements about the *absolute* magnitudes of G_A and G_V, or rather of G_G and G_F. To verify even qualitatively the universality of the "$V-xA$" interaction, one must show that $G_G/G_F \simeq -1$.

It has been pointed out[10] that the hyperfine (hf) effect in muon capture, i.e., the difference in the capture rates for the $F=0$ and $F=1$ hyperfine states of the mesonic hydrogen atom in (1), is particularly sensitive to the ratio G_G/G_F. Accepting conclusion (a) above, and assuming that the observed capture rate in liquid hydrogen is, after some corrections, essentially that for the $F=0$ atom, one can, indeed, conclude that this ratio has the negative sign required by UFI.

There is, however, another approach: To observe the hf effect in muon capture by complex nuclei. In fact, as was shown by Bernstein, Lee, Yang, and Primakoff[11] (BLYP), the hf effects just mentioned should persist, with observable magnitudes, when the muon is captured by a light nucleus, in particular by a nucleus that consists of a closed shell plus a "lone" proton. BLYP, assuming that there is no transition between the two hf states (F_+,F_-), suggested an experiment which could possibly exhibit that a $I=0$ nucleus was capturing with two incoherent rates, but not show which of these, F_+ or F_-, was capturing *faster*; this is, however, precisely the information needed to establish the ratio G_G/G_F. Telegdi[12] showed that an atomic conversion process, of rate R at least comparable to the difference in capture rates $\Delta\Lambda$, connects F_+ and F_-, and emphasized that the influence of this transition on the time distribution of decay electrons ("negative curvature") could be exploited to infer the *sign* of $\Delta\Lambda$. It was subsequently shown[13] that the R estimates of reference 12 were in error, and predicted $R \gg \Delta\Lambda$ quite generally, and, in particular, for Al^{27}. This was consistent with the experimental evidence[14] (absence of curvature) of the time distribution of μ-decay electrons from Al^{27}. It was also shown in reference 13 that while $R \gg \Delta\Lambda$ made *electron* rate experiments on spin dependence very difficult if not impossible, the same condition leads to particularly large effects in the time distribution of *capture products*. As will be shown in detail later (Sec. IV), this enables one to determine $\Delta\Lambda$ in a very direct manner, virtually without extra assumptions. While the *quantitative* connection between $\Delta\Lambda$ and the coupling constants is still subject to the uncertainties of nuclear physics, such experiments have the virtue that the capture rates in *both* hf states, as well as the conversion process, are directly *observed*; in the case of liquid hydrogen, the conversion process has to be postulated and a long chain of μ molecular ion physics arguments goes into interpreting the experimental result.

Experiments on the hyperfine effect have been performed in this laboratory by observing the time distributions both of the neutral capture products and of the decay electrons from F^{19} (the ideal target nucleus for such effects). Brief descriptions of these experiments, which convincingly show that "$V-xA$" (rather than "$V+xA$") with $x \approx 1$ holds in muon capture as required by UFI, have already appeared.[15,16] The purpose of the present paper is: (i) to give a detailed account of the calculations of the conversion rate R (Sec. III), (ii) to present a survey of the possible hf experiments with complex nuclei (Sec. IV), and (iii) to discuss critically the F^{19} experiments just referred to (Secs. V through VII). The theory underlying the spin dependence of muon capture is summarized in Sec. II, and finally our conclusions are presented in Sec. VIII.

II. SUMMARY OF THEORY OF hf EFFECTS IN MUON CAPTURE

Let the μ-capture interaction be described by an equivalent nonrelativistic Hamiltonian

$$H = G_F(1^{(b)} \cdot 1^{(l)} - x\boldsymbol{\sigma}^{(b)} \cdot \boldsymbol{\sigma}^{(l)}), \tag{2}$$

the only form possible neglecting terms proportional to $\mathbf{v}$, the neutrino momentum. Here $-x = G_G/G_F$, the ratio of the (nonrelativistic equivalent) Gamow-Teller to Fermi coupling constants. The capture rates in hydrogen ($Z=1$, $A=1$) are given by

$$\Lambda_0^{\text{cap}}(1,1) \sim \langle \mu p, F=0 \,|H|\, \nu n\rangle^2 = G_F^2(1+3x)^2, \tag{3a}$$

$$\Lambda_1^{\text{cap}}(1,1) \sim \langle \mu p, F=1 \,|H|\, \nu n\rangle^2 = G_F^2(1-x)^2, \tag{3b}$$

while the spin-averaged rate is

$$\bar{\Lambda}^{\text{cap}}(1,1) \equiv \tfrac{1}{4}(3\Lambda_1^{\text{cap}} + \Lambda_0^{\text{cap}}) \sim G_F^2(1+3x^2) = (G_F^2 + 3G_G^2). \tag{4}$$

The spin-dependence, i.e., hf effect, can be characterized by

$$\frac{\Delta\Lambda}{\bar{\Lambda}^{\text{cap}}}(1,1) \equiv \frac{\Lambda_0^{\text{cap}} - \Lambda_1^{\text{cap}}}{\bar{\Lambda}^{\text{cap}}} = \frac{8x(x+1)}{1+3x^2}. \tag{5}$$

As is evident from (3) and (5), $x=+1$ (the situation corresponding most closely to UFI) leads to the maximum hf effect, with $\Lambda_1^{\text{cap}}(1,1)=0$, while $x=-1$ leads to zero hf effect, though formally the interaction (2) is still spin-dependent. Note that a pure GT interaction ($|x| \to \infty$) yields $\frac{2}{3}$ as large an effect (5) as the UFI type ($x \approx +1$) coupling.

[10] Ya. B. Zel'dovich and S. S. Gershtein, Usp. Fiz. Nauk **71**, 581 (1960) [translation: Soviet Phys.—Usp. 3, 593 (1961)].
[11] J. Bernstein, T. D. Lee, C. N. Yang, and H. Primakoff, Phys. Rev. **111**, 313 (1958).
[12] V. L. Telegdi, Phys. Rev. Letters **3**, 59 (1959).
[13] R. Winston and V. L. Telegdi, Phys. Rev. Letters **7**, 104 (1961).
[14] J. F. Lathrop, R. A. Lundy, V. L. Telegdi, R. Winston, and D. D. Yovanovitch, Phys. Rev. Letters **7**, 107 (1961).
[15] G. Culligan, J. F. Lathrop, V. L. Telegdi, R. Winston, and R. A. Lundy, Phys. Rev. Letters **7**, 458 (1961).
[16] R. A. Lundy, W. A. Cramer, G. Culligan, V. L. Telegdi, and R. Winston, Nuovo Cimento **24**, 549 (1962).

Before deriving formulas equivalent to (5) for complex nuclei (Z,A), we first amend our hydrogen estimate for the omission of the "induced pseudoscalar" term in the Hamiltonian (2). This contributes[1] a term $-G_P[(\boldsymbol{\sigma}^{(b)}\cdot\boldsymbol{\nu}/|\boldsymbol{\nu}|)\,(\boldsymbol{\sigma}^{(l)}\cdot\boldsymbol{\nu}/|\boldsymbol{\nu}|)]$ to the interaction, where G_P is the relevant equivalent coupling constant. In analogy with (4), one obtains

$$\bar{\Lambda}^{\mathrm{cap}}(1,1)\sim(G_F^2+3\Gamma_G^2), \tag{6}$$

where

$$\Gamma_G^2\equiv G_G^2+(G_P^2-2G_GG_P)/3, \tag{7}$$

so that it is convenient to define

$$-X\equiv\Gamma_G/G_F. \tag{8}$$

With assumptions of UFI, one computes[1] $X=1.23$, a value very close to that of x $(=1.21)$ generally assumed to hold in β decay. In terms of X, the analog of (5) can be cast into the convenient form

$$\frac{\Delta\Lambda}{\bar{\Lambda}^{\mathrm{cap}}}(1,1)=\frac{8}{1+3X^2}\left\{X(X+1)-\left[X\left(1-\frac{G_G}{\Gamma_G}\right)+\frac{1G_P}{3G_F}\left(\frac{G_P}{G_F}-1\right)\right]\right\}. \tag{9}$$

In view of the preceding remarks, the purely X-dependent term has almost exactly the value that a naive application of (5) would have given; the second term is small, and in particular, for the UFI choice of parameters, amounts only to a 6% correction. (N. B.: this correction term is not sensitive to the sign of X, i.e., it remains small even for $X\approx-1$.)

Following BLYP,[11] the estimates (5) or (9) are extended to complex nuclei by considering a nucleus of charge Z and spin I consisting of a spinless "core" of charge $(Z-1)$ and a "lone" proton occupying an $l_{I\pm1/2}$ orbital. By a simple Landé-type argument relating the proton and muon spins, one readily gets ($\Lambda_\pm^{\mathrm{cap}}$ = capture rates in the $F_\pm$ states, $\Delta\Lambda\equiv\Lambda_-^{\mathrm{cap}}-\Lambda_+^{\mathrm{cap}}$)

$$\frac{\Delta\Lambda}{\bar{\Lambda}^{\mathrm{cap}}}(Z,A)=\frac{1}{4}\frac{\Delta\Lambda}{\bar{\Lambda}^{\mathrm{cap}}}(1,1)\times\frac{1}{\bar{Z}}$$

$$\times\begin{cases}(2I+1)/I, & \text{if } I=l+\tfrac{1}{2} \quad (10a)\\ -(2I+1)/(I+1), & \text{if } I=l-\tfrac{1}{2}. \quad (10b)\end{cases}$$

Here

$$\bar{\Lambda}^{\mathrm{cap}}\equiv[(I+1)\Lambda_+^{\mathrm{cap}}+I\Lambda_-^{\mathrm{cap}}]/(2I+1), \tag{11}$$

is defined in analogy with (4), while

$$\bar{Z}\equiv(Z-1)\xi+1. \tag{12}$$

The parameter ξ (≤1) is introduced[11] to allow for the possibility that the Pauli exclusion principle has a stronger inhibitory effect for the "core" than for the lone proton. The main uncertainty in the predictions (10) comes from the difficulty in predicting ξ. Aside from this, it is, however, clear, both from (10) and from physical intuition, that the lightest nucleus with one $s_{1/2}$ proton outside a saturated core will yield the largest hf effect, i.e., constitute the ideal "pseudohydrogen." This nucleus is F^{19}, which has a magnetic moment right on the Schmidt line for an $s_{1/2}$ proton.[17]

An actual estimate for ξ, i.e., of the influence of nuclear physics on the magnitude of the hf effect (10), can be obtained in several ways. Primakoff[18] has, with some mild assumptions, evaluated his *exact* closure formulas (i.e., including terms of order $1/Z$, contrary to the discussion in reference 1) for the hf effect, and obtains—for an $s_{1/2}$ proton (or hole) outside (inside) a $J=0$, $T=0$ core—the expression[19]

$$\frac{\Delta\Lambda}{\bar{\Lambda}^{\mathrm{cap}}}(Z,A)=\left\{\frac{1}{4}\frac{\Delta\Lambda}{\bar{\Lambda}^{\mathrm{cap}}}(1,1)\frac{1}{Z}\right\}\times\frac{[1-\alpha(A-Z)/2]}{[1-\alpha(A-1)/2Z-\alpha(A-Z)/2]}, \tag{13}$$

where the braced term is the BLYP estimate (10) for $\xi=1$, and the new parameter α can be extracted from the observed mean rates $\bar{\Lambda}^{\mathrm{cap}}(Z,A)$ through the relation

$$\alpha\approx\delta[(A-Z)/2A][(A-1)/2Z+(A-Z)/2]^{-1}, \tag{14}$$

while[1] $\bar{\Lambda}^{\mathrm{cap}}(Z,A)\sim[1-\delta(A-Z)/2A]$; the best fit[5] to the observed capture rates over a wide range of Z and A yields

$$\delta=3.13. \tag{15}$$

For F^{19}, (14) gives with (15) $\alpha=0.137$, i.e., an increase of 1.8 over the BLYP estimate. The estimate (13) can readily be extended to the case of a nucleus of isotopic spin T, where several protons (holes) are outside (inside) a $J=0$, $T=0$ core, e.g., Cl^{37}. One simply has to replace the term $(A-1)/2Z$ in Eqs. (13) and (14) by $(A-2T)/2Z$, allowing in the BLYP term for the altered spin correlation conditions.

By assigning a specific shell-model wave function (including configuration mixing) one can, of course, work out the mean capture rate and hf effect for any given nucleus. The latter was done by Überall[20] for

[17] The $s_{1/2}$ assignment to F^{19}, so attractive from a naive point of view, is actually doubtful because it requires the $2s$ shell to be filled before the $1d$ shell. A proper mixed wave function for the ground state has been given by M. G. Redlich, Phys. Rev. **99**, 1427 (1955). This wave function forms the basis of Überall's calculation, reference 19.

[18] H. Primakoff (unpublished private communication to V. L. Telegdi).

[19] The exact evaluation of Eq. (27a) of reference 1 gives for the case considered,

$$\frac{\Delta\Lambda}{\bar{\Lambda}^{\mathrm{cap}}}(Z,A)=\left\{\frac{1}{4}\frac{\Delta\Lambda}{\bar{\Lambda}^{\mathrm{cap}}}(1,1)\frac{1}{Z}\right\}\times\frac{\{\xi_a-[(A-Z)/2]\alpha_a'^{(-)}\}}{\{1-[(A-Z)/2Z]\alpha_a'^{(+)}-[(A-Z)/2]\alpha_a^{(-)}\}},$$

while Eq. 8 of reference 1 yields $\delta[(A-Z)/2A]=[(A-1)/2Z]\times\alpha_a^{(+)}+[(A-Z)/2]\alpha_a^{(-)}$. The approximation consists in taking $\xi_a\approx1$ and $\alpha_a'^{(-)}\approx\alpha_a^{(-)}\approx\alpha_a^{(+)}\equiv\alpha$.

[20] H. Überall, Phys. Rev. **121**, 1219 (1961).

F^{19}, Al^{27}, and P^{31}. In the case of F^{19}, Überall's and Primakoff's estimate, Eq. (13), coincide, while in the two other cases (see Table II, Sec. IV) the agreement is less good. In view of the limited success of shell-model calculations[21] of $\bar{\Lambda}^{\rm cap}(Z,A)$, it is not clear why Überall's estimates should be considered more reliable than Primakoff's.

III. CALCULATION OF CONVERSION RATES

The purpose of this section is to see in which mesonic atoms transitions within the hyperfine doublet can take place by internal conversion (electron ejection) and to estimate the conversion rates. We will confine the discussion to odd-Z, odd-A nuclei with one proton in the outer shell[22] since these fit the model of a core+lone proton best.

The source of both splitting and conversion is the hyperfine structure (hfs) interaction; for the case of two particles described by s-state wave functions about a common origin, this interaction can be described by the equivalent nonrelativistic Hamiltonian[23]

$$H=-(8/3)\pi\boldsymbol{\mu}_1\cdot\boldsymbol{\mu}_2\delta(\mathbf{r}_1-\mathbf{r}_2), \tag{16}$$

where $\boldsymbol{\mu}_1$, $\boldsymbol{\mu}_2$ are the respective magnetic moments. The hfs splitting of the mesonic atom is given by

$$\epsilon=\int\int H\Psi_p{}^2(\mathbf{r}_1)\Psi_\mu{}^2(\mathbf{r}_2)d^3r_1d^3r_2, \tag{17}$$

where Ψ_p, Ψ_μ are the outer proton, muon s-state wave functions, respectively. In ordinary atomic hfs the departure of the nuclear charge distribution from a point nucleus can be treated as a perturbation[24]; in the mesonic case such a treatment is, however, not appropriate since the muon Bohr radius and the nuclear radius may become comparable in magnitude. No new computations are, however, required to evaluate (17) exactly, because the quantity

$$Z_{\rm eff}{}^4\equiv\pi a_0{}^3\left[\sum_p\int\Psi_p{}^2(\mathbf{r})\Psi_\mu{}^2(\mathbf{r})d^3r\right], \tag{18}$$

where a_0 is the muon Bohr radius and the sum is taken over all protons, plays an important role in muon capture and has already been computed numerically for most nuclei by Ford and Wills.[25] The reason that essentially the same volume integral intervenes in hfs and muon capture is that the latter interaction has the same $\delta(\mathbf{r}_1-\mathbf{r}_2)$ character as (16). From Eqs. (16) through (18) we obtain[26]

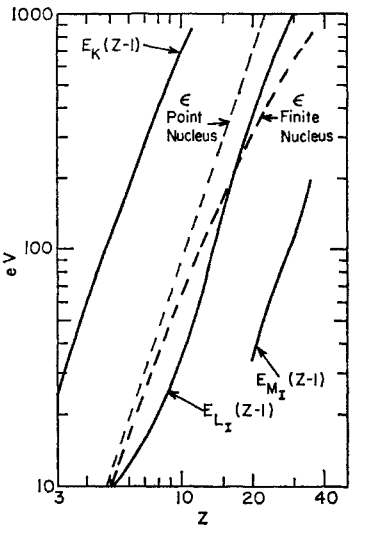

FIG. 1. Mesonic atom hfs splittings for $\mu_I=1$, $I=\frac{1}{2}$ compared with the binding energies of their electron shells. Point nucleus values are for $Z_{\rm eff}\equiv Z$, finite nucleus for $Z_{\rm eff}$ as defined in Eq. (18).

$$\epsilon=\frac{Z_{\rm eff}{}^4}{Z}\frac{2}{3}\alpha^2m_p{}^{-1}m_\mu{}^2\frac{(2I+1)}{I}\mu_I$$

$$=0.04715\frac{(2I+1)}{I}\frac{Z_{\rm eff}{}^4}{Z}\mu_I\ \text{eV}, \tag{19}$$

where μ_I is measured in Bohr magnetons. In giving Eq. (19) for arbitrary I we anticipate the result, discussed below, that this estimate applies approximately (to better than $\approx 20\%$) to $I>\frac{1}{2}$ nuclei as well.

For the hyperfine transition to take place by internal conversion, ϵ must clearly exceed the binding energy of the converting shell. In Fig. 1, ϵ and the binding energies of the various atomic shells are plotted vs Z, putting $\mu_I=1$ and $I=\frac{1}{2}$ in (19) to obtain a qualitative survey of the situation. This survey is confined to $Z\lesssim 35$, because the hf effects in muon capture decrease as $1/Z$ and hence lose experimental interest for large Z, say 35. Figure 1 shows that the hf splitting is never large enough to cause K conversion and always sufficient to eject the M electrons. In the L shell the situation is less clear cut: One may generally expect conversion for $Z\lesssim 15$, but for $Z>15$ the possibility of conversion will depend on the specific values of I and μ_I as well as on details of nuclear structure.

In borderline cases, i.e., where ϵ appears to lie near the threshold for ionizing a particular shell, we must refine our estimate (19). The treatment given so far is valid strictly for s-state protons. Bohr and Weisskopf[27] have already discussed, for the atomic case, the dependence of ϵ on the details of nuclear magnetization, i.e., the differing contributions of the orbital and spin magnetic moments of the nucleus. There are two

[21] H. A. Tolhoek and J. R. Luyten, Nucl. Phys. 3, 679 (1957); G. H. Burkhardt and C. A. Caine, Phys. Rev. 117, 1375 (1960).

[22] The extension to several protons in an outer shell is straightforward; one simply sums our expressions over the protons in the shell.

[23] Our treatment will be nonrelativistic throughout since only low-Z nuclei and slow ($v/c\ll\alpha Z$) electrons are involved.

[24] H. Kopfermann, *Nuclear Moments* (Academic Press Inc., New York, 1958), 2nd ed.

[25] K. W. Ford and J. G. Wills, Los Alamos Scientific Laboratory Report LAMS 2387, 1960 (unpublished).

[26] We use atomic units: $[m]=m_e$, $[l]=\hbar^2/me^2$, $[t]=\hbar^3/me^4$ and the unit of energy $=2$ Ry≈ 27.2 eV.

[27] A. Bohr and V. F. Weisskopf, Phys. Rev. 77, 94 (1950).

effects: (a) The orbital magnetic moment contribution to the energy ϵ is increased by a relative amount Δ_l; (b) the spin contribution is decreased [because $\Psi_p(\mathbf{r})$ is no longer isotropic] by a relative amount $\zeta\Delta_l$. We reproduce for convenience the nonrelativistic reduction of the Bohr-Weisskopf formulas:

$$\Delta_l=\left\langle -\int\left(\frac{r'}{r}\right)^3\frac{d}{dr'}\Psi_\mu^2(r')dr'\right\rangle\Big/\langle\Psi_\mu^2(r)\rangle, \quad (20)$$

$$\zeta=(2I-1)/4(I+1) \quad \text{for} \quad I=l+\tfrac{1}{2},$$

$$\zeta=(2I+3)/4I \quad \text{for} \quad I=l-\tfrac{1}{2},$$

where the brackets denote an average over $\Psi_p^2(r)$, the proton density. To apply these corrections in practice one needs to know how much of the nuclear moment μ_I is due to spin (μ_s) and how much to orbital motion (μ_l). If one assumes that the departure of μ_I from the Schmidt value is due to configuration mixing of single-particle proton states, the desired decomposition is

$$\begin{aligned}\mu_l&=(g_sI-\mu_I)/(g_s-1),\\ \mu_s&=g_s(\mu_I-I)/(g_s-1),\end{aligned} \quad (21)$$

where $g_s=5.59$ is the proton g factor. These Bohr-Weisskopf effects are fairly small ($\Delta_l\approx 2\%$ for $Z=6$, $\approx 10\%$ for $Z=30$),[28] but afflicted, for the reason just given, with considerable uncertainty.[28a] Fortunately, it turns out that there is only one borderline case of physical interest, viz., Cl^{35}. For this nucleus, ϵ is presumably increased from 120 to 145 eV, but still lies below the $L_{\rm I}$ edge, 163.6 eV (see Table I). One could, in principle, turn the argument around and by experimentally determining whether Cl^{35} does or does not convert in the L shell obtain information about the distribution of nuclear magnetization. At the high-Z end of Table I, there are other borderline cases, but for these the conversion is probably too rapid (>300 μsec^{-1}) and the hf effects too small to be experimentally useful.

We now discuss the calculation of the conversion rates; its results are summarized in Table I. The total rate in a mesonic atom is given by

$$R=\sum R_{nlj\to klj}, \quad (22)$$

where the sum is taken over all ionizable shells, the indices have their usual significance, and k stands for a continuum state. The s-shell conversion rate follows directly from the Hamiltonian (16). The nucleus and $1s$ muon can be considered as a "pseudonucleus" of charge $Z'\equiv Z-1$ and magnetic moment

$$\boldsymbol{\mu}'=m_p^{-1}\frac{\mu_I}{I}\mathbf{I}+m_\mu^{-1}\tfrac{1}{2}\boldsymbol{\sigma}_\mu. \quad (23)$$

For the atomic electron, this "pseudonucleus" is point-like, and $\mathbf{r}_1$ can be taken as the origin, yielding

$$R_{ns\to ks}=\frac{4}{9}\pi\alpha^4m_\mu^{-2}\frac{I}{(2I+1)}\left(1+\frac{m_\mu}{m_p}\frac{\mu_I}{2I}\right)^2\times u_{ns}^2(0)\,|u_{ks}(0)|^2\rho(k), \quad (24)$$

where u_{ns}, u_{ks} are the bound and continuum radial wave functions and $\rho(k)$ the density of final states of the ejected electron. For p-shell conversion the Hamiltonian corresponding to (16) takes the nonrelativistic form

$$H=\tfrac{1}{2}\boldsymbol{\mu}_1\cdot[l_e-\tfrac{1}{2}\boldsymbol{\sigma}_e+\tfrac{3}{2}r^{-2}(\boldsymbol{\sigma}_e\cdot\mathbf{r})\mathbf{r}]\mathbf{r}^{-3}, \quad (25)$$

which gives for the conversion rates

$$R_{np_{\frac{1}{2}}\to kp}=\frac{4}{9}\pi\alpha^4m_\mu^{-2}\frac{I}{(2I+1)}\left(1+\frac{m_\mu}{m_p}\frac{\mu_I}{2I}\right)^2\times\left(\frac{33}{2}\right)\left|\int_0^\infty u_{np}r^{-3}u_{kp}r^2dr\right|^2\rho(k), \quad (26)$$

$$R_{np_{\frac{3}{2}}\to kp}=\frac{4}{9}\pi\alpha^4m_\mu^{-2}\frac{I}{(2I+1)}\left(1+\frac{m_\mu}{m_p}\frac{\mu_I}{2I}\right)^2\times\left(\frac{69}{10}\right)\left|\int_0^\infty u_{np}r^{-3}u_{kp}r^2dr\right|^2\rho(k). \quad (27)$$

Here u_{np}, u_{kp} have an obvious significance, the fractions (33/2) and (69/10) arise from angular integrals; they can be worked out by elementary methods, or be taken from Rose.[29] The rates (24), (26), (27) are already summed over the electrons of the pertinent shells, assumed to be filled. We shall generally assume that the holes created by Auger ejection during the cascade of the muon down to the $1s$ state are replenished in a time short compared to $1/R$. The persistence of such holes in the electron shells could decrease R by (a) depleting electrons that would otherwise be available for conversion, and (b) raising above threshold the binding energy of a shell that would otherwise be expected to convert. The presence of holes would also lead to a rapid depolarization of the muon in its K shell. We will return to this point in the next section.

The conversion processes we are discussing here are entirely analogous to the internal conversion of nuclear $M1$ transitions. Internal conversion has been treated exhaustively by Rose[29]; the reason that we do not simply take over his results is that one is here concerned

[28] Using muon wave functions and nuclear charge distributions of K. W. Ford and J. G. Wills (reference 25 and private communication).

[28a] *Note added in proof.* A detailed calculation of mesonic atom hfs splittings in Al^{27}, Ta^{181}, and Bi^{209} has been made by M. LeBellac [Laboratoire des Physique Théorique et Hautes, Energies, Faculté des Sciences, Orsay France]. For Al^{27} this author finds $\epsilon=250$ eV while our simple estimate [Eq. (19)] gives 263 eV (see Table I) which the Bohr-Weisskopf effects [Eq. (20)] increase to 270 eV.

[29] M. E. Rose, *Internal Conversion Coefficients* (Interscience Publishers, Inc., New York, 1958).

TABLE I. Conversion calculations.

Element	μ_I[a]	Odd-proton configuration[b]	Z_{eff}/Z[c]	ϵ (eV)	Lowest ejected shell (eV)	$u_{ns}^2(0)$ estimate[h]	$u_{ns}^2(0)$ Hartree[i]	R' (μsec^{-1})	R (μsec^{-1})
B^{11}	2.69	$(p_{3/2}^3)_{3/2}$	≈110	18	$L_I(9.3)$[d]	7.6	9.1	3.5×10^{-6}	0.25
F^{19}	2.63	$(s_{1/2}^{-1})$	532	126	$L_I(30)$[e]	83	96	1.1×10^{-3}	5.8
Na^{23}	2.22	$(d_{5/2}^3)_{3/2}$	905	120	$L_I(40)$[e]	170	182	1.0×10^{-3}	1.4×10^{1}
Al^{27}	3.64	$(d_{5/2}^{-1})$	1345	263	$L_I(88.6)$[f]	370	400	1.2×10^{-2}	4.1×10^{1}
P^{31}	1.13	$(s_{1/2}^{-1})$	1886	190	$L_I(150)$[f]	680	735	2.9×10^{-3}	5.8×10^{1}
Cl^{35}	0.82	$(d_{3/2})$	2446	120	$M_I(5)$[g]	71	···	9.1×10^{-4}	8.0
Cl^{37}	0.68	$(d_{3/2})$	2446	98	$M_I(5)$[g]	71	···	4.9×10^{-4}	8.0
K^{39}	0.39	$(d_{3/2}^3)_{3/2}$	3085	72	$M_I(35)$[g]	121	174	1.9×10^{-4}	2.2×10^{1}
Sc^{45}	4.76	$(f_{7/2})$	≈3800	920	$L_I(439)$[f]	2510	2575	5.2×10^{-1}	4.6×10^{2}
V^{51}	5.15	$(f_{7/2}^3)_{7/2}$	4635	1220	$L_I(565)$[f]	3500	···	1.2	7.0×10^{2}
Mn^{55}	3.47	$(f_{7/2}^5)_{5/2}$	5335	995	$L_I(699)$[f]	4730	4520	6.3	9.3×10^{2}
Co^{59}	4.65	$(f_{7/2}^{-1})$	≈6000	1450	$L_I(850)$[f]	6220	5700	2.0	1.3×10^{3}
Cu^{63}	2.23	$(p_{3/2})$	6912	925	$L_{II}(872)$[f]	8000	···	4.6×10^{-1}	5.0×10^{2}
Ga^{69}	2.02	$(p_{3/2}^3)_{3/2}$	≈7500	900	$M_I(132)$[f]	1560	1430	4.2×10^{-1}	3.3×10^{2}
Ga^{71}	2.56	$(p_{3/2}^{-1})$	7500	1150	$L_{II}(1040)$[f]	10000	9650	9.0×10^{-1}	6.5×10^{2}
As^{75}	1.43	$(p_{3/2}^{-1})$	8400	720	$M_I(175)$[g]	2040	1800	1.9×10^{-1}	4.3×10^{2}
Br^{79}	2.11	$(p_{3/2}^{-1})$	≈9000	1150	$M_I(227)$[g]	13000	···	8.8×10^{-1}	3.4×10^{3}
Br^{81}	2.27	$(p_{3/2}^{-1})$	≈9000	1200	$M_I(227)$[g]	13000	···	1.0	3.4×10^{3}

[a] N. Ramsey, *Nuclear Moments* (John Wiley & Sons, Inc., New York, 1960), p. 78.
[b] J. H. C. Jensen, in *Beta- and Gamma-Ray Spectroscopy*, edited by Kai Siegbahn (Interscience Publishers, Inc., New York, 1955), p. 430.
[c] See reference 60; interpolated values are indicated by ≈.
[d] C. E. Moore, N. B. S. Circular 467 (1949).
[e] Hartree estimate (see reference 30).
[f] D. H. Tomboulian, in *Handbuch der Physik*, edited by S. Flügge (Springer-Verlag, Berlin, 1957), Vol. 30, p. 246.
[g] R. D. Hill, E. L. Church, and J. W. Mihelich, Rev. Sci. Inst. 23, 523 (1952).
[h] Estimated using Eq. (31); n is the principal quantum number of the lowest ejected shell.
[i] Hartree estimate (see reference 30); n is the principal quantum number of the lowest ejected shell.

with very low energies ($\epsilon \lesssim$ keV, see Fig. 1), well outside the range considered by Rose.

The problem in evaluating the conversion rate consists in obtaining reliable values of the electron wave functions u_{nl}. The bound-state term $u_{ns}^2(0)$ enters into atomic hfs and can, for outer shells, occasionally be extracted from hfs and Knight shift data.[12] Generally, the dominant contribution to R comes, however, from the inner shells ($n=2$, 3). For these we can either use the Hartree wave functions available for many atoms,[30] or else estimate $u_{ns}^2(0)$ by a method familiar from atomic hfs. This method makes use of a heuristic argument due to Goudsmit,[31] justified through the J.W.K.B. method by Fermi and Segrè,[32] which goes as follows: in a semiclassical theory of atomic hfs the quantity that intervenes in the energy is $\langle r^{-3}\rangle_{\text{av}}$, the time average of r^{-3} over the electron motion. In the absence of screening, this has the hydrogenoid value; to include screening, Goudsmit considers the motion in two regions, viz., in an inner region (in) where the electron sees the bare nuclear charge $Z=Z_{\text{in}}$, and in an outer region (out) where that charge is screened. Letting $\langle r_{\text{in}}^{-3}\rangle_{\text{av}}$, $\langle r_{\text{out}}^{-3}\rangle_{\text{av}}$ be the time averages of r^{-3} in the corresponding regions and τ_{in}, τ_{out} the times spent in each region, one has

$$\langle r_{\text{in}}^{-3}\rangle_{\text{av}} = (\langle r_{\text{in}}^{-3}\rangle_{\text{av}}\tau_{\text{in}} + \langle r_{\text{out}}^{-3}\rangle_{\text{av}}\tau_{\text{out}})/(\tau_{\text{in}}+\tau_{\text{out}}) \approx r_{\text{in}}^{-3}\tau_{\text{in}}/\tau_{\text{out}}. \quad (28)$$

This approach is useful because the quantities in these distinct regions can be estimated from the hydrogenic case with nuclear charge Z_{in}, Z_{out}, respectively. Quantum mechanically, $\langle r^{-3}\rangle_{\text{av}}$ gets replaced by $\langle r^{-3}\rangle$; this expression cannot be evaluated for s states, where it diverges.[33] This difficulty is overcome by noting that the correct hfs Hamiltonian for s states [i.e., Eq. (16)] is proportional to $\delta(\mathbf{r}-0)$ rather than to r^{-3} so that the analog of Eq. (28) for s states is

$$u_{ns}^2(0) \approx [u_{ns}^2(0)]_{\text{in}}\tau_{\text{in}}/\tau_{\text{out}} \approx 4Z_{\text{in}}Z_{\text{out}}^2/n^3, \quad (29)$$

where the last equality follows from $[u_{ns}^2(0)]_{\text{in}}\tau_{\text{in}} \approx 4Z_{\text{in}}$, $\tau_{\text{out}} \approx n^3/Z_{\text{out}}^2$. In our case, $Z_{\text{in}}=Z'$, the pseudonuclear charge, while Z_{out} follows from approximating the energy levels of the screened atom by the hydrogenoid form

$$E_n \approx -(Z'-S_n)^2/2n^2 + V_{0n}; \quad (30)$$

here S_n, V_{0n} are Slater inner, outer screening constants for the ns shell.[34] Therefore, our estimate for the bound-state term in (24) is

$$u_{ns}^2(0) \approx 4Z'(Z'-S_n)^2/n^3. \quad (31)$$

Table I shows that the simple estimate (31) agrees quite well (to better than 15%) with available Hartree estimates over the entire Z range considered.

The foregoing considerations may also be used to estimate the effect of screening on the continuum term $|u_{ks}(0)|^2\rho(k)$. We observe that the inner region terms

[30] R. S. Knox, in *Solid State Physics*, edited by F. Seitz and D. Turnbull (Academic Press Inc., New York, 1957), Vol. 4, p. 413.
[31] S. Goudsmit, Phys. Rev. 43, 636 (1933).
[32] E. Fermi and E. Segrè, Reale Accademia D'Italia 4, 131 (1933).
[33] It is remarkable that one nevertheless obtains the correct hf energy for s states by evaluating $\langle r^{-3}\rangle$ for $l>0$ and then putting $l=0$ in the general formula.
[34] J. C. Slater, Phys. Rev. 36, 57 (1930).

correspond to an unscreened atom, while $\tau_{\text{out}} \approx \tau$ the period for screened motion, so that (29) may be expressed by

$$[u_{ns}^2(0)\tau]_{\text{screened atom}} \approx [u_{ns}^2(0)\tau]_{\text{unscreened atom}}. \quad (32)$$

For continuum states, τ is replaced by $2\pi\rho(k)$ so that one would anticipate in analogy with (32)

$$[|u_{ks}(0)|^2\rho(k)]_{\text{screened atom}} \approx [|u_{ks}(0)|^2\rho(k)]_{\text{unscreened atom}} \approx 4Z', \quad (33)$$

where the last equality is correct for the small energies $k^2/2 \ll Z'^2/2$ that are of interest. The validity of (33) has been justified through the J.W.K.B. method by Rose[35] except for a fine point to which we shall return below. In fact, Rose showed that for (33) to hold, it is sufficient that $k^2/2 \ll (Z'^2/2 + V_0)$; here V_0, the outer screening constant in the vicinity of $r=0$, can be estimated as the difference between the unscreened and observed K-shell binding energies, i.e., $V_0 \approx Z'^2/2 - E_K(Z')$. It is apparent from Fig. 1 that this condition on $k^2/2$ is fulfilled.

Using Eqs. (31) and (33) we have

$$R_{ns\to ks} = \frac{16}{9}\pi\alpha^4 m_\mu^{-2} \frac{I}{(2I+1)}\left(1+\frac{m_\mu}{m_p}\frac{\mu_I}{2I}\right)^2 u_{ns}^2(0)Z'$$
$$= \frac{I}{(2I+1)}\left(1+\frac{m_\mu}{m_p}\frac{\mu_I}{2I}\right)^2 u_{ns}^2(0)Z' \times 1.53\times 10^4 \text{ sec}^{-1}, \quad (34)$$

$$R_{ns\to ks} \approx \frac{64}{9}\pi\alpha^4 m_\mu^{-2} \frac{I}{(2I+1)}\left(1+\frac{m_\mu}{m_p}\frac{\mu_I}{2I}\right)^2 \frac{(Z'-S)^2 Z'^2}{n^3}$$
$$= \frac{I}{(2I+1)}\left(1+\frac{m_\mu}{m_p}\frac{\mu_I}{2I}\right)^2 \frac{(Z'-S_n)^2 Z'^2}{n^3} \times 6.13\times 10^4 \text{ sec}^{-1}. \quad (35)$$

Where the result for $R_{ns\to ks}$ has been given both without and with the explicit estimate (31) for $u_{ns}^2(0)$ to emphasize that a Hartree calculated value for $u_{ns}^2(0)$ is to be preferred over (31).

In any given shell, s conversion dominates, and p conversion, Eqs. (26) and (27), becomes important only when ϵ happens to fall between the binding energies of the two subshells, say L_{I}, L_{II}. In these cases, $k^2/2 \ll V_0$, and one can give an explicit expression for the matrix element in complete analogy with Goudsmit's formula, viz.,

$$\left|\int_0^\infty u_{np} r^{-3} u_{kp} r^2 dr\right|^2 \rho(k) \approx \frac{(Z'-S_n)^2 Z'^2}{9n^3}. \quad (36)$$

In this estimate we assume that because of the r^{-3} term, most of the contribution comes from the vicinity of the origin, and one ignores $k^2/2$ compared to V_0. [$k^2/2$ is indeed less than V_0 for most nuclei, e.g., $\approx (1/3)V_0$ in F^{19} so that this is not a severe restriction.]

We then have

$$R_{np\to kp} \approx 0.11 R_{ns\to ks}, \quad (37)$$

$$R_{np_{\frac{1}{2}}\to kp} \approx 0.05 R_{ns\to ks}. \quad (38)$$

Rose's proof of the Goudsmit formula for continuum s states [Eq. (33)] requires that $(k^2 - V_0)$ be positive, a situation that obtains for nuclear transitions but not, in general, for the small hf splittings of mesonic atoms. To verify that (33) holds for negative $(k^2 - V_0)$ as well, we outline a quantum-mechanical proof of Goudsmit's formula.[36]

Let the potential region in which the electron moves be divided into an inner region where there is no inner screening,

$$V_{\text{in}}(r) = -Z'/r + V_0, \quad (39)$$

and an outer region, $r > r_0$ say, where r_0 is chosen large enough ($>1/Z'$) to allow a J.W.K.B. solution

$$u_{\text{out}}(r) = (C/p_r^{1/2}) \sin\left[\int_{r_0}^{r} p_r dr + \text{phase}\right]; \quad (40)$$

here

$$C = [2\pi\rho(k)]^{-1/2}, \quad (41)$$

while the other terms in (40) have their usual significance. From (39) it follows that $u(0)/u(r_0)$ can be taken from the pure Coulomb case with energy $k'^2/2 \equiv (k^2/2 - V_0)$ (and a small energy change does not matter); then taking $u(r_0)$ from Eq. (40), with (41), gives

$$u_{ks}^2(0)\rho(k) = 4Z', \quad \text{for} \quad k'^2/2 \ll Z'^2/2. \quad (42)$$

Equation (42) holds for $k'^2/2$ of either sign; near threshold, however, the condition on $k'^2/2$ is no longer maintained as $k'^2/2 \approx -V_0$ which is comparable in magnitude to $Z'^2/2$. However, Fermi and Segrè[32] have shown by explicitly joining the inner solution to the J.W.K.B. solution that Eq. (42) holds quite accurately even for *bound* states ($k^2/2 < 0$). Therefore, (42) may be considered valid down to threshold.

To make connection with the literature we define an internal conversion coefficient

$$\beta \equiv R/R', \quad (43)$$

where R' is the $M-1$ radiation rate between hfs states, given by

$$R' = \frac{4}{3}\alpha^5 m_\mu^{-2} \frac{I}{(2I+1)}\left(1+\frac{m_\mu}{m_p}\frac{\mu_I}{2I}\right)^2 \epsilon^3$$
$$= \frac{I}{(2I+1)}\left(1+\frac{m_\mu}{m_p}\frac{\mu_I}{2I}\right)^2 \epsilon^3 \times 26.6 \text{ sec}^{-1}. \quad (44)$$

The quantity β is introduced in nuclear physics because it alone is subject to calculation. In mesonic atoms, R and R' are individually calculable while β, which is always very large (>400) because of the small energies involved, is not particularly useful.

Since ratios between conversion coefficients of the various shells change more slowly with energy than the coefficients themselves[29] we compare the lowest ϵ and Z' data from reference 29 with our estimates.

For $Z'=25$, $\epsilon = 25$ keV $\approx 3Z'^2/2$, reference 29 gives

[35] M. E. Rose, Phys. Rev. **49**, 727 (1936).

[36] I am grateful to Professor G. Wentzel for helpful suggestions for this proof.

$\beta_{2s}/\beta_{1s}=0.087, \beta_{2p_{1/2}}/\beta_{2s}=0.048, \beta_{2p_{3/2}}/\beta_{2p_{1/2}}=0.38$ while we get for $\epsilon \ll \frac{1}{2}Z'^2$, $\beta_{2s}/\beta_{1s}=0.096$, $\beta_{2p_{1/2}}/\beta_{2s}=0.11$, $\beta_{2p_{3/2}}/\beta_{2p_{1/2}}=0.45$. At the same time, the magnitude of β_{1s} say, is a factor ≈ 4 larger than given by reference 29 (after allowing for the ϵ^{-3} dependence). We note the following points:

(a) All the odd-Z, odd-A, mesonic atoms from $Z=5$ to $Z=35$ covert at a rate $R \gg \Lambda^{\text{cap}}$ (and, therefore, $\gg \Delta\Lambda$ independently of the muon capture mechanism). This makes the originally proposed hf experiments[11] on the electron decay rate very difficult (effects of order $\Delta\Lambda/R$) but favors the hf effect on the rate of neutral products (neutrons and/or γ rays) from muon capture (for F^{19} one has a 36% effect).

(b) For $5 \leq Z \leq 19$, R is small enough (compared with $\Lambda^{\text{cap}}+\Lambda^{\text{dec}}$) to make experiments attractive. For higher Z, R is probably too large ($>300\ \mu\text{sec}^{-1}$) to make the detection of departures in the time distribution (from a pure exponential) of either capture products or electrons practical. We will now proceed to formulate these conclusions quantitatively.

IV. SURVEY OF EXPERIMENTALLY OBSERVABLE hf EFFECTS

Granting the high ($R \gg \Delta\Lambda$) conversion rates, we now derive some of their observable consequences.

A. Time Distribution, $N_{n/\gamma}(t)$, of Neutral Capture Products ("Neutrals")

As an aid to this and the subsequent discussion, consider Fig. 2: At $t=0$, the time of their arrival in the mesonic K shell, muons populate the $F_\pm$ states statistically, i.e.,

$$\begin{aligned} n_+(0) &= (I+1)/(2I+1), \\ n_-(0) &= I/(2I+1). \end{aligned} \tag{45}$$

Let $\alpha_{n/\gamma}$ be the probability for detecting a neutron and/or γ ray per muon capture. Then the rate of "neutrals" observed per muon at $t=0$ is

$$N_{n/\gamma}(0)=\alpha_{n/\gamma}\bar{\Lambda}^{\text{cap}}, \tag{46}$$

where $\bar{\Lambda}^{\text{cap}}$ is the F-averaged capture rate

$$\bar{\Lambda}^{\text{cap}} \equiv n_+(0)\Lambda_+^{\text{cap}}+n_-(0)\Lambda_-^{\text{cap}}. \tag{47}$$

For times $\gg R^{-1}$, the muon population has dropped by conversion into the F_- state so that one has (Λ_- = total disappearance rate from the F_- state)

$$N_{n/\gamma}(t \gg R^{-1})=\alpha_{n/\gamma}\Lambda_-^{\text{cap}}e^{-\Lambda_- t}. \tag{48}$$

Since the $t=0$ rate must go over to the asymptotic one with a time constant R^{-1}, one has for all t

$$N_{n/\gamma}(t) \approx \alpha_{n/\gamma}\Lambda_-^{\text{cap}}(1-A_{n/\gamma}e^{-Rt})e^{-\Lambda_- t}, \tag{49}$$

where

$$A_{n/\gamma} \equiv (1-\bar{\Lambda}^{\text{cap}}/\Lambda_-^{\text{cap}})=n_+(0)\Delta\Lambda/\Lambda_-^{\text{cap}}. \tag{50}$$

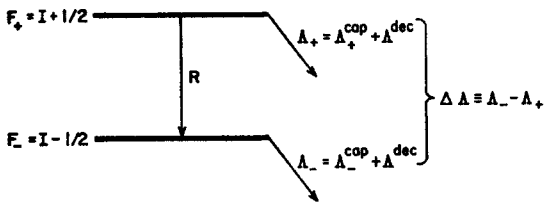

FIG. 2. Mesonic atom hyperfine doublet. The channels for conversion (R), capture ($\Lambda_\pm^{\text{cap}}$) and decay (Λ^{dec}) are indicated assuming $\mu_I>0$.

This expression neglects terms of order $\Delta\Lambda/R$ which as we have seen are very small. $A_{n/\gamma}$ vs Z are tabulated in Table II using the estimates given in Sec. II. To get an idea of the magnitude of $A_{n/\gamma}$, we tentatively replace Λ_-^{cap} by $\bar{\Lambda}^{\text{cap}}$ in Eq. (10a), and obtain for an $I=l+\frac{1}{2}$ nucleus

$$A_{n/\gamma} \approx (I+1)/IZ. \tag{51}$$

This can be a large effect for small Z and I (e.g., $\approx \frac{1}{3}$ in F^{19}).

Up to now, we have made the physically plausible assumption that $\alpha_{n/\gamma}$ is the same for both hyperfine states (i.e., that there are no branching ratio effects). This assumption could fail, for example, because of differences in the multiplicites or energy spectra of the capture product in question. Distinguishing the α's for the two hf states by suitable indices, the effective contribution of the F_+ state will be increased by a factor α_+/α_-, and A will be changed by a relative amount

$$\Delta A/A=(\alpha_+/\alpha_--1)\Lambda_+^{\text{cap}}/\Delta\Lambda. \tag{52}$$

Clearly, such a change need not be identical for n's and γ's, so that one could have $A_n \neq A_\gamma$, contrary to Eq. (50). This makes it desirable to determine A_n and A_γ separately.

B. Time Distribution, $N_e(t)$, of Decay Electrons

One sees right away that using the above reasoning one would predict a pure exponential for the decay electron rate. This means that the hyperfine effect on the electrons is of order $\Delta\Lambda/R$, i.e., negligibly small to the order of approximation of the preceding section. To determine $N_e(t)$ we again compare the rate at $t=0$ with the rate for $t \gg R^{-1}$,

$$N_e(0)=\alpha_e\Lambda^{\text{dec}}, \tag{53}$$

where α_e is essentially the fractional solid angle seen by the electron detector. If $\Delta\Lambda/R$ were exactly $=0$ (instant conversion) one would have for all $t>0$

$$N_e(t)=\alpha_e\Lambda^{\text{dec}}e^{-\Lambda_- t}. \tag{54}$$

However, $\Delta\Lambda/R$ is finite, and for a time $\sim R^{-1}$ a fraction of the muons $\approx n_+\Delta\Lambda/R$ is saved (for $\Delta\Lambda>0$), producing an additional activity at long times of

$$\delta N_e(t)=\alpha_e\Lambda^{\text{dec}}n_+(0)(\Delta\Lambda/R)e^{-\Lambda_- t}. \tag{55}$$

TABLE II. Estimates of hyperfine effects.

Element	Λ_-^{cap} (μsec^{-1})[a]	$\Delta\Lambda/\bar{\Lambda}^{cap}$	$A_{n/\gamma}$	$A_e\times10^2$	$D_{n/\gamma}$	D_e
B^{11}	0.01	0.51[b]	0.24	0.96	...	...
B^{11}	0.01	1.2[c]	0.43	1.7	...	...
F^{19}	0.24	0.42[b]	0.24	1.0	1.0	3.0×10^1
F^{19}	0.24	0.76[c]	0.36	1.5	...	...
F^{19}	0.24	0.76[d]	0.36	1.5	...	...
Na^{23}	0.38	0.14[b]	0.08	0.22	1.9×10^1	2.1×10^3
Al^{27}	0.66	0.18[b]	0.09	0.14	7.5×10^1	4.5×10^4
Al^{27}	0.66	0.28[c]	0.14	0.22	...	...
Al^{27}	0.66	0.49[d]	0.22	0.35	...	...
P^{31}	1.12	0.25[b]	0.16	0.31	3.8×10^1	2.5×10^4
P^{31}	1.12	0.37[c]	0.22	0.42	...	...
P^{31}	1.12	0.45[d]	0.25	0.48	...	...
Cl^{35}	1.38	−0.09[b]	−0.06	−1.0	4.1	4.7×10^1
Cl^{37}	1.38	−0.09[b]	−0.06	−1.0	4.1	4.7×10^1
Cl^{37}	1.38	−0.14[c]	−0.10	−1.7	1.9×10^1	7.5×10^2
K^{39}	1.99	−0.08[b]	−0.05	−0.54	>104	$>10^{11}$
K^{39}	1.99	−0.11[c]	−0.07	−0.07	>104	$>10^{11}$
Sc^{45}	≈2.4	0.10[b]	0.05	0.05	>104	$>10^{11}$
V^{51}	3.27	0.09[b]	0.04	0.02	>104	$>10^{11}$
V^{51}	3.27	0.13[c]	0.07	0.03	>104	$>10^{11}$
Mn^{55}	3.90	0.06[b]	0.03	0.01	>104	$>10^{11}$
Co^{59}	≈4.5	0.08[b]	0.04	0.01	>104	$>10^{11}$
Cu^{63}	5.97	0.09[b]	0.05	0.06	>104	$>10^{11}$
Ga^{69}	≈5.8	0.08[b]	0.04	0.07	>104	$>10^{11}$
Ga^{71}	≈5.8	0.08[b]	0.04	0.04	>104	$>10^{11}$
As^{75}	≈6.2	0.08[b]	0.04	0.06	>104	$>10^{11}$
Br^{79}	≈7.0	0.07[b]	0.03	0.006	>104	$>10^{11}$
Br^{81}	≈7.0	0.07[b]	0.03	0.006	>104	$>10^{11}$

[a] Weighted mean values of capture rates measured to date; ≈ indicates values interpolated on the Primakoff plot (see reference 60).
[b] BLVP estimate, Eq. (10); the demerit factors are based on this estimate as it is the only one available for all elements.
[c] Primakoff estimate, Eq. (13).
[d] Überall's shell-model estimate.

It follows that one has for all t (to first order in $\Delta\Lambda/R$)

$$N_e(t)=\alpha_e\Lambda^{dec}[1+n_+(0)(\Delta\Lambda/R)(1-e^{-Rt})]e^{-\Lambda_- t}, \quad (56)$$

which can be cast into the convenient form

$$N_e(t)\sim(1-A_e e^{-Rt})e^{-\Lambda_- t}, \quad A_e\equiv n_+(0)\Delta\Lambda/R. \quad (57)$$

From Eqs. (50) and (57) we see that the electron and neutral effects are in the ratio

$$A_e/A_{n/\gamma}=\Lambda_-^{cap}/R, \quad (58)$$

i.e., very unfavorable to the electron experiment. However, the latter has the advantage of being free of possible branching ratio effects, since Λ^{dec} is the same in both F states. Values of A_e, based on Eq. (57) are given in Table II. Note that since both "neutrals" and electron effects are linear in $\Delta\Lambda$, they reverse sign when one goes from $l+\frac{1}{2}$ nuclei to $l-\frac{1}{2}$ nuclei,[37] i.e., $A_{n/\gamma}$ and A_e are positive for $l+\frac{1}{2}$ nuclei (e.g., F^{19}) but negative for $l-\frac{1}{2}$ nuclei (e.g., Cl^{35}, Cl^{37}).

C. Effects of Muon Polarization

We now drop the assumption that the muons are unpolarized. Since this has important consequences for $N_e(t)$, we discuss this distribution first.

While there is no direct effect of the muon polarization on A_e, the asymmetry of the electron decays (of the form $1+a\cos\theta$) can seriously alter the *observed* A_e. Here, θ is the angle between the incoming muon and decay electron momenta and a the asymmetry coefficient. Consider first $I=\frac{1}{2}$, for which a is expected to be largest. At $t=0$, $a=a(\frac{1}{2})$, the usual F-averaged asymmetry coefficient for $I=\frac{1}{2}$. Assuming no hyperfine depolarization of the muon *during* its cascade to the K shell, well-known arguments predict[38,39]

$$a(\tfrac{1}{2})=(\tfrac{1}{2})a(0), \quad (59)$$

where $a(0)$ is the asymmetry coefficient for $I=0$ (≈-0.04). For $t\gg R^{-1}$ the muons will have dropped to the isotropic $F=0$ state so that $a=0$. Let $N_e^{F(B)}(t)$ be the electron rate for $\theta=0(\pi)$; it readily follows that

$$N_e^{F(B)}(t)\sim(1-A_e^{F(B)}e^{-Rt})e^{-\Lambda_- t}, \quad (60)$$

where

$$A_e^{F(B)}=A_e-(+)a(\tfrac{1}{2}) \quad (61)$$

to first order in a and in $\Delta\Lambda/R$.

Measuring A_e^F and A_e^B determines both the hyperfine effect $n_+(0)\Delta\Lambda/R$ and the F-averaged decay asymmetry, a. Because of the rapid conversion this method for measuring asymmetry for $I=\frac{1}{2}$ nuclei has some advantages over the usual one of precessing the muon spin in an external magnetic field; in the latter method rather high fields may be required to turn the muon

[37] I am indebted to Professor Telegdi for pointing this novel effect out to me.

[38] V. L. Telegdi, *Proceedings of the International Conference on Mesons and Recently Discovered Particles, Padua-Venice, September 22–28, 1957* (Società Italiana di Fisca, Padua-Venice, 1958).

[39] H. Überall, Phys. Rev. 114, 1640 (1959).

spin by more than one turn in a time $\sim R^{-1}$ (e.g., >700 G for F^{19}). For arbitrary I, simple recoupling arguments show that

$$a(I)=\tfrac{1}{3}a(0)[1+\tfrac{1}{2}(I+\tfrac{1}{2})^{-2}]. \quad (62)$$

For $t\gg R^{-1}$, the residual asymmetry in the F_- state is contributed both by muons initially populating the F_- state and by muons dropped by conversion to the F_- state. Since in an F_+ to F_- transition the muon spin is flipped, these two contributions would cancel each other in the large-I limit. For finite I, the cancellation is not complete and one shows by a simple recoupling argument that

$$a/a(0)=-\tfrac{1}{3}a(0)g(I)(I+\tfrac{1}{2})^{-2}, \quad (63)$$

where

$$g(I)\equiv(I+\tfrac{1}{2})(I+\tfrac{3}{4})(I+\tfrac{1}{2})^{-1}$$

and we have assumed that a $j=\frac{1}{2}$ electron is ejected (i.e., neglected $p_{3/2}$ conversion). It follows from Eqs. (62) and (63) that

$$A_e{}^{F(B)}=A_e-(+)[a(0)/3][1+(I+\tfrac{1}{2})^{-2}(\tfrac{1}{2}+g(I))] \quad (64)$$

for the general case.

Table II shows that because of the smallness of A_e, the asymmetry contribution is either of the same order as A_e ($a\approx-0.02$, $A_e\approx0.015$ in F^{19}) or dominates the effect.

Since an asymmetry in the angular distribution of neutrons from muon capture (of the form $1+\alpha\cos\theta$) is predicted theoretically and has been observed in $I=0$ nuclei,[6-8] it is of interest to see to what extent such asymmetries affect $N_n(t)$.

We use the BLYP model and restrict ourselves to $I=\frac{1}{2}$. For arbitrary I, the reader is referred to Überall's general discussion.[39] At $t=0$ neutrons from capture by the $Z'(\equiv Z-1)$ core have an asymmetry parameter $\alpha(0)/2$, where $\alpha(0)$ is the neutron asymmetry parameter for an $I=0$ nucleus. [$a(0)\approx-0.03$.[6-8]] Capture by the lone proton gives $\bar{\alpha}(1,1)$, the F-averaged asymmetry from hydrogen capture. Weighting the core by $Z'\xi$, one has

$$\alpha=\frac{Z'\xi\alpha(0)/2+\bar{\alpha}(1,1)}{(Z'\xi+1)}, \quad t=0. \quad (65)$$

For $t\gg R^{-1}$, there is no asymmetry as only the $F=0$ state is populated.

Therefore,

$$A_n{}^{F(B)}=A_n-(+)\frac{Z'\xi\alpha(0)/2+\bar{\alpha}(1,1)}{(Z'\xi+1)}, \quad (66)$$

where we have used notation already introduced.

To get an explicit estimate we set $\xi=1$.

$$A_n{}^{F(B)}\approx A_n-(+)(1/Z)[Z'\alpha(0)/2+\bar{\alpha}(1,1)]. \quad (67)$$

Primakoff[1] gives $\bar{\alpha}(1,1)/\alpha(0)\approx-0.01$ *assuming* a "universal $V-xA$" interaction.

Then one has,

$$A_n{}^{F(B)}\approx A_n+(-)0.015, \quad I=\tfrac{1}{2}. \quad (68)$$

The large-I limit is

$$A_n{}^{F(B)}\approx A_n+(-)\alpha(0)/3\approx A_n+(-)0.01. \quad (69)$$

For the favorable hyperfine experiments that will be discussed later, these asymmetry effects are small ($\lesssim20\%$). Note that the γ's from muon capture show no asymmetry.[7]

It has been suggested by Ignatenko *et al.*[40] that these conclusions need to be modified in the case of the two allotropic forms (red and black) of phosphorus. Ignatenko *et al.*[40] propose that in red phosphorus (an insulator) holes in the outer shells resulting from Auger ejection during the mesonic cascade have a lifetime much longer than the muon lifetime τ_μ, while in black phosphorus (a semiconductor) the refilling time of these holes is supposedly short compared to τ_μ. The presence of about 4 holes would be sufficient to push the L_I edge above threshold for L_I (i.e., $2s$) conversion ($\epsilon=190$ eV). This idea is advanced in support of some experimental results of the Dubna group[41] that muons stopped in red phosphorus yield the asymmetry $a(\frac{1}{2})$ expected for an $I=\frac{1}{2}$ nucleus in the absence of fast conversion (i.e., $a\cong-0.02$), but that muons in black phosphorus exhibit *no* decay asymmetry. One can raise two objections to the arguments of reference 40:

(1) The unfilled holes postulated by reference 40 would, in general (i.e., except when exactly two electrons of opposite spin were missing), have net magnetic moments which would rapidly depolarize the muon, resulting in no observable asymmetry.[42]

(2) Even with 4 holes in the M shell, the binding energy of the remaining $2p$ electrons in phosphorous would be about 150 eV,[43] i.e., $<\epsilon=190$ eV. $2p$ conversion would occur at about 16% of the $2s$ rate [see Eqs. (37), (38)], i.e., $R_{2p}\approx8\times10^6$ sec^{-1}, as compared to $\tau_\mu(P^{31})=0.6$ μsec. It is clear that our estimate of R_{2p} need be only qualitatively correct to ensure a rapid disappearance of the decay asymmetry in any kind of phosphorus. (N.B.: Since P^{31} is an $s_{1/2}$ nucleus and the $2p$ conversion occurs near threshold, both our energy and rate estimates should be reliable.)

Finally, it must be mentioned that we have looked for a decay asymmetry in red phosphorus in this laboratory and obtained a zero result.[44]

---

[40] A. E. Ignatenko, I. G. Petrashku, and D. Chultem, Dubna Report D-823, 1961 (unpublished).

[41] L. B. Egorov, C. V. Zhuravlev, A. E. Ignatenko, A. V. Kuptsov, Li Hsuan-ming, and M. G. Petrashku, Zh. Experim. i Teor. Fiz. **41**, 684 (1961) [translation: Soviet Phys.—JETP **14**, 494 (1962)].

[42] I am indebted to Professor V. L. Telegdi for this argument.

[43] H. L. Donley, Phys. Rev. **50**, 1012 (1936).

[44] J. F. Lathrop, R. A. Lundy, V. L. Telegdi, and R. Winston (to be published).

D. Choice of Target Elements

In order to select the elements most suitable for experiments on hyperfine effects in muon capture, it is useful to characterize them by a demerit factor D. This D will be proportional to the number of muons, N_μ, that one would have to stop in order to measure A [Eqs. (50) and (62)] to some preassigned accuracy. There are two considerations: (1) the statistical one of relating the variance of A [$\equiv\sigma^2(A)$] to the number of events, N; (2) the purely instrumental problem of measuring a time distribution without distortions close to $t=0$. We consider the statistical problem first, i.e., a fit of the data to an expression like

$$f(t)=C(1-Ae^{-Rt})e^{-\Lambda_- t}. \tag{70}$$

(We neglect for purposes of discussion the presence of a background term.) The discussion is simplified by the fact that all the nuclei of interest except B^{11} satisfy, in addition to $R\gg\Delta\Lambda$, the stronger condition $R\gg\Lambda_-$. Disregarding, for the time being, B^{11}, this means that $t\lesssim R^{-1}$ events which alone convey significant information about (CA) and R are only a small fraction $\sim(\Lambda_-/R)$ of the total. Most of the data ($t\gtrsim R^{-1}$) are available for determining C and Λ_-. It follows that the variance in C is given by

$$\sigma^2(C)/C^2\approx 2/N. \tag{71}$$

Similarly, the variance in (CA) is given by

$$\sigma^2(CA)/(CA)^2\approx 2(R/\Lambda_-)/(NA^2). \tag{72}$$

Therefore, from Eqs. (71) and (72)

$$\sigma^2(A)\approx 2(R/\Lambda_-)/N. \tag{73}$$

In addition, one has

$$N/N_\mu\approx\epsilon_{n/\gamma}\Lambda_-^{\rm cap}/\Lambda_-, \quad \text{for "neutrals",} \tag{74a}$$

$$N/N_\mu\approx\epsilon_e\Lambda^{\rm dec}/\Lambda_-, \quad \text{for decay electrons.} \tag{74b}$$

Combining Eqs. (73) and (74) we find

$$D_{n/\gamma}\sim A_{n/\gamma}^{-2}(R/\Lambda^{\rm cap}), \quad \text{for "neutrals,"} \tag{75a}$$

$$D_e\sim(\epsilon_{n/\gamma}/\epsilon_e)A_e^{-2}(R/\Lambda^{\rm dec})\approx 0.1A_e^{-2}(R/\Lambda^{\rm dec}), \quad \text{for electrons,} \tag{75b}$$

where $(\epsilon_{n/\gamma}/\epsilon_e)\approx 0.1$ is based on *observed* "efficiency" for "neutrals" in the experiment described in Sec. V.

Next, to allow for instrumental distortion of the time distribution for $0<t<\Delta t$, we multiply D by a factor $e^{2R\Delta t}$ and tentatively assign $\Delta t\approx 20$ nsec since this is a practical lower limit set by the fastest digital time analyzer (100 Mc/sec "digitron") currently available.[45]

A glance at the demerit factors listed in Table II shows that F^{19} is the optimal choice for both "neutrals" and electron experiments. (The D's have been normalized to $D_{n/\gamma}(F^{19})\equiv 1$ to facilitate comparison.) This choice coincides with the one made in Sec. II, on the basis of muon-capture theory considerations. The isotopes Cl^{35} and Cl^{37} follow fairly closely in order of demerit.[46] We recall that Cl^{35} and Cl^{37} are $l-\frac{1}{2}$ nuclei and should have *negative* $A_{n/\gamma}$ and A_e in contrast to F^{19}. The elements K^{19}, Na^{23}, P^{31}, and Al^{27} are one to two orders of magnitude less favorable than F^{19} for hyperfine experiments.

The elements for $Z>19$ are many orders of magnitude more difficult than F^{19} and, hence, probably of no immediate interest. B^{11} is an interesting special case. For this target, R is slow compared to Λ_- ($R/\Lambda_-=0.55$) and one has for the "neutrals" a nonexponential decay extending over several boron lifetimes. Such a long-time departure of $N_n(t)$ from a pure exponential is best characterized by the logarithmic curvature, K.[12] For B^{11} K is so large (≈ -0.24) that the *apparent* lifetime of the "neutrals" as determined, say, by the Peierls method[47] exceeds the true B^{11} lifetime (as would essentially be measured from the electron rate) by $\approx 13\%$. Fig. 3 illustrates this point. We note that since these boron effects are functions of A_n and R, they give A_n only once R is known or computed from theory. This is in contrast with the $R\gg\Lambda_-$ case, where one obtains both A_n and R without assumptions.

V. "NEUTRALS" EXPERIMENT[48]

A. Beam and Counting Arrangement

The arrangement of counters is shown in Fig. 4(a). A "π^-" beam of 150-MeV/c momentum was obtained from the Chicago Synchrocyclotron. The pions were produced in a vibrating Be target[49] yielding a low (≈ 5) duty factor. The μ^-'s (comprising about 5% of the total beam) were separated from the π^-'s by range; a Lucite Čerenkov counter, 3, in anticoincidence, reduced the effective e^- contamination to about 20%

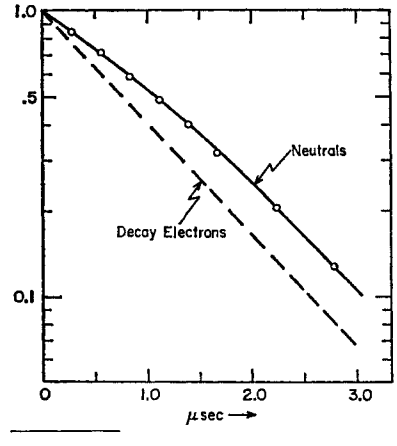

FIG. 3. Predicted hf effect in B^{11} "neutrals." The decay-electrons time distribution is essentially exponential with very nearly the free-muon lifetime; the "neutrals" time distribution is nonexponential with an *apparent* lifetime $\approx 13\%$ greater than that of the decay electrons.

[45] R. A. Lundy, Rev. Sci. Instr. **34**, 146 (1963).

[46] Note, however, that our R estimate for Cl^{35} may be too low for the reasons given in Sec. III.

[47] R. Peierls, Proc. Roy. Soc. (London) **A149**, 467 (1935).

[48] For a preliminary account of this experiment, see reference 15.

[49] J. Rosen, Bull. Am. Phys. Soc. **6**, 9 (1961).

of the stopped μ^-. With 23-g/cm^2 of copper moderator placed ahead, 3 was sensitive to e^- only. Except as noted, this beam description applies to all measurements described in this paper.

The μ^- entered the apparatus through a 6-in.-square hole in a 2-ft-thick Pb wall closed off by counter 1. They passed through a beam-defining counter 2, followed by a Pb collimator with a 3-in. aperture, were moderated by copper, traversed Čerenkov counter 3, counters 4 and 5, and stopped in a 6-g/cm^2 LiF target T (LiF powder compressed to a density of $\rho \approx 1.5$ and encased in a 1/32-in. wall Lucite box). Since $\Lambda^{\text{cap}}(\text{Li})$ is negligible compared to $\Lambda^{\text{cap}}(\text{F})$, their ratio being $\approx 7\times 10^{-3}$, LiF constitutes a convenient "fluorine" target for capture measurements. The front and back faces of the target were covered by counters 8 and 5; the remaining four sides were covered by yoke-shaped counters 6 and 7 positioned symmetrically above and below T. This configuration of counters 5 through 8 completely enclosing the target will be referred to as a "house." A stopped muon was identified by a $(2\bar{3}45\bar{8})$ coincidence. In addition the "house" was put into slow (5 μsec) anticoincidence with the arriving muon in order to suppress events accompanied by decay electrons from the target. The "neutrals" detector, counter 9, was a 5-in.-deep by 5-in.-diam glass tank filled with liquid scintillator[50] and coupled to an RCA 7046 photomultiplier. The signature of a "neutrals" event was a $(\bar{1}\bar{8}9)$ coincidence. Furthermore, a pulse-shape discrimination circuit (psd) following 9 enabled one to distinguish between n- and γ-induced events. Except for 3 and 9 the counters were plastic scintillators and all but 9 were coupled to their photomultipliers by ultraviolet-transmitting Lucite light pipes. The coincidence circuits employed were of Garwin design[51] with a resolution of about 20 nsec.

B. Measurement of $N_{n/\gamma}(t)$

The counting logic is shown schematically in Fig. 4(b). The time intervals between stopped muon and "neutrals" (n/γ) events were measured with a digital instrument ("digitron")[52,53] that recorded their distribution $[N_{n/\gamma}(t)]$ in the memory of a 400-channel pulse-height analyzer (PHA). Each channel had a width of 50 nsec, i.e., the digitron was operated at 20 Mc/sec. For a complete description of this digitron and its calibration procedure, the reader is referred to Lundy's exhaustive article.[53] Routing pulses from the pulse-shape discrimination circuit (psd) caused the events to be recorded in appropriate, distinct subsections of the PHA memory, permitting the simultaneous measurement of $N_n(t)$ and $N_\gamma(t)$.[54] If an event was accompanied

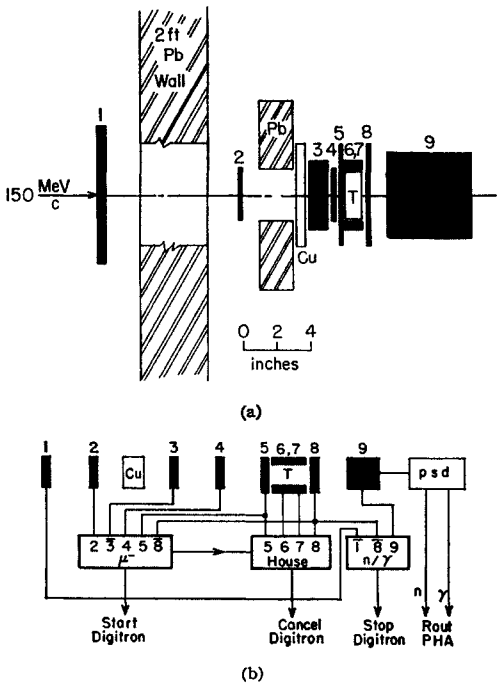

FIG. 4 (a). Experimental arrangement for "neutrals" experiment. 1, 2, 4, 5, 6, 7, 8, plastic scintillators, viz., $1=8\times 8\times \frac{1}{2}$ in., $2=3\times 3\times \frac{1}{4}$ in., $4=3\times 3\times \frac{1}{4}$ in., $5=6\times 6\times \frac{1}{8}$ in., $8=6\times 6\times \frac{1}{4}$ in., 6 and 7 yoke-shaped and enclose a target T from above and below; 3, $4\times 4\times 1$ in. Lucite Čerenkov counter; 9, 5-in.-deep by 5-in.-diam liquid scintillator counter followed by pulse-shape discriminator (psd); Cu, moderator; Pb, collimators; T, LiF target. (b). Block diagram of "neutrals" experiment. $(2\,\bar{3}\,4\,5\,\bar{8})$ = "muon" signature; $(\bar{1}\,\bar{8}\,9)$+psd = neutron or gamma signature; an output from any "house" counter (5, 6, 7, or 8) during 5 μsec following a "muon", cancels the event.

by an output from the "house," signalling a muon decay, its storage in the PHA was suppressed. The function of the "house" will be discussed in some detail later.

C. Performance of the Pulse-Shape Discrimination Circuit

The pulse-shape discrimination circuit (psd), designed by J. F. Lathrop[55] in this laboratory, was patterned after the ideas of Brooks and Owen.[56] Its performance was tested with neutrons from a Po-Be source and with 2.61-MeV γ's from ThC. By setting the energy threshold at ≈ 1.7-MeV γ energy (corresponding to a recoil proton energy, E_p, of ≈ 4.5 MeV), a rejection efficiency of $\approx 97\%$ for γ-induced pulses between threshold and 2.61 MeV was achieved. This efficiency improves with energy until the energy deposited is large enough ($\gtrsim$10–15 MeV) to saturate the photomultiplier. This same circuit had been used here previously to observe the asymmetry of neutrons from μ capture.[7]

It is useful to compare the actually observed neutron yield with a theoretical estimate. The expected neutron

[50] NE213 liquid scintillator; composition $C_6H_4(CH_3)_2$; Nuclear Enterprises, Winnipeg, Canada.
[51] R. L. Garwin, Rev. Sci. Instr. 24, 618 (1953).
[52] R. A. Swanson, Rev. Sci. Instr. 31, 149 (1960).
[53] R. A. Lundy, Phys. Rev. 125, 1686 (1962).
[54] In some early runs, no n, γ discrimination was made, and we simply recorded $N_n(t)+N_\gamma(t)$.
[55] Present address: University of Illinois, Urbana, Illinois.
[56] F. D. Brooks, Nucl. Instr. Methods 4, 151 (1959); R. B. Owen, I. R. E. Trans. Nucl. Sci. 5, 198 (1958).

yield is given by

$$Y_n=\eta(\Lambda_-^{\text{cap}}/\Lambda_-)(\Omega/4\pi)\epsilon_n, \tag{76}$$

where η is the neutron multiplicity per muon capture, Ω the mean solid angle subtended by counter 9, and ϵ_n the efficiency for neutron detection. We estimate ϵ_n by a semianalytical method due to Hardy,[57] assuming a theoretical neutron spectrum as predicted for O^{16} by Dolinsky and Blokhintsev.[58] This procedure neglects edge effects, i.e., approximates our cylindrical counter by a semi-infinite slab and, therefore, gives an overestimate. For the scintillator used [$C_6H_4(CH_3)_2$] and an energy threshold of $E_p\approx 4.5$ MeV, we estimate (taking $\eta=1$) that $\epsilon_n\approx 30\%$, i.e., $\alpha_n\approx 0.50\%$ with $\Omega/4\pi\approx 5.5\%$, while the observed α_n was $\approx 0.35\%$. This theoretical estimate is yet uncorrected for muon stops in Li. The LiF electron experiment to be described in Sec. VIII indicates that about 18% of the muons stopped in Li; this tends to improve the agreement between the predicted and observed yields. One expects α_n to be a rapidly decreasing function of the energy threshold; in fact, both the *theoretical* and *observed* α_n were found to decrease by about 40% when this threshold was raised from 1.5 to 2.0 MeV. The qualitative agreement between the estimated and observed α_n's implies (granting the theoretical neutron spectrum) that the neutron multiplicity η in muon capture by F^{19} is not drastically different from 1. As to the γ yield, the observed α_γ was of the same order as α_n.

D. Backgrounds; Role of the "House"

In view of the anticipated low yield of true neutron events ($\approx 0.35\%$), the sources of background required special attention. The function of the "house" was to prevent the recording of events accompanied by decay electrons. A muon coincidence ($2\bar{3}45\bar{8}$) generated a 5-μsec gate. If an output pulse from any of the four "house" counters 5, 6, 7, or 8 fell within this gate, the corresponding event was not stored. In addition, sufficient delay was added to counters 6, 7, and 8 to insure that events due to muons stopping in the "house" were not stored, thus preventing the "house" from becoming effectively part of the target. The efficiency of the "house" for counting decay electrons was checked by stopping μ^+'s in the target and measuring the time distribution of the e^+'s counted by the "house." From this, an efficiency of 80% was inferred.

(a) *Accidental Background*

This is due to neutral events in the tank uncorrelated with the stopping muons. With the "house" operative, one should "look" for "neutrals" only when no decay occurred; ideally, this should reduce this type of background by a factor of $(\Lambda_-/\Lambda_-^{\text{cap}})\approx 2.9$. Allowing for the finite "house" efficiency (80%) and the e^- contamination of the beam ($\approx 20\%$ of the muon stops), the expected reduction is ≈ 2.1, in good agreement with the measured value of $2.2+0.2$. Counter 1, which closed off the hole in the Pb wall and was traversed by all particles entering the setup, was further put into anticoincidence with 9 to reduce accidentals. It is convenient to characterize the amount of accidental background by a figure of merit λ,[47] defined to be the ratio of true to background events at zero time. At a muon stop rate of ≈ 200/sec, the λ was ≈ 50 for $N_n(t)$ and ≈ 15 for $N_\gamma(t)$. Suitable logic as described by Lundy[53] was provided within the digitron to reject multistart and multistop events, thus insuring that the accidental background time spectrum was flat.

(b) *Bremsstrahlung from Decay Electrons*

Decay electrons directed at 9 were anticoincidenced by 8 covering its face. However, decay electrons not directed at 9 could radiate in the target and be detected as "neutrals" via their γ rays. This bremsstrahlung would follow the time distribution of the decay electrons (an almost pure exponential) and, hence, tend to dilute the "neutrals" effect predicted in Eq. (50). The "house," by eliminating decay electron events, helped to suppress this source of background. The efficiency for counting bremsstrahlung from decay electrons was checked by stopping μ^+'s in the target and looking for *neutral products*. We found $\gamma/\mu\approx 0.06\%$, $n/\mu\approx 0.01\%$, which are both well below the level of the true "neutrals" yields of 0.35% (the finite *neutron* yield is evidence for saturation effects in counter 9 at high γ energies). With the "house" off, the bremsstrahlung contribution was seen to increase by a factor ≈ 2.5. Operating without the "house" would have seriously decreased the observed effect in $N_\gamma(t)$.

(c) *Carbon Background*

In decay-electron counting experiments, carbon background from muons stopping and decaying in counter wrappings and dead layers can constitute a serious problem.[14] In an experiment such as this, where capture products are counted, carbon contamination is suppressed by a factor $\Lambda^{\text{cap}}(F)/\Lambda^{\text{cap}}(C)\approx 5$ and is, therefore, not significant ($<1\%$ at $t=0$).

E. Data Analysis and Control Runs

Three sets of data were collected, viz., $N_n(t)$, $N_\gamma(t)$, and $N_{n\gamma}(t)$, the latter consisting of data obtained without the psd requirement as well as of the sum of the first two sets. The data were analyzed in two stages as suggested in the discussion of demerit factors. First, the late ($t>0.5$ μsec) part of each set was fitted to $f(t)=Ce^{-\Lambda_- t}+B$ for C, Λ_-, and B, where B is the accidental background. Using the value of Λ_- so

[57] J. E. Hardy, Rev. Sci. Instr. **29**, 705 (1958).
[58] E. I. Dolinsky and L. D. Blokhintsev, Nucl. Phys. **10**, 527 (1959).

obtained, the total data was then fitted to

$$f(t)=C(1-Ae^{-Rt})e^{-\Lambda_- t}+B$$

for C, CA, R, and B. Because of the finite digitron resolution (two-channels wide) and an anticoincidence "hole" ($\approx$30 nsec) near $t=0$, the first two channels after $t=0$ (0.1 μsec) were omitted from the analysis. Since one requires the value of A at $t=0$ in order to compare it with theory, Eq. (50), the fitted $f(t)$ was extrapolated to $t=0$. Clearly, one needs to know for this purpose the position of $t=0$ to better than a channel width. This was measured by recording the $t=0$ events generated by particles passing through both μ and n/γ telescopes, i.e., by switching off the anticoincidence counters 1 and 8 and removing the Cu moderator. The resolution function shape of digitron[53] is such that a $\delta(t-0)$ distribution of events falls into two adjacent channels. The weighted mean of the occupation numbers of these gives $t=0$. In general, the $t<0$ time spectrum recorded by digitron can be used to infer B.[53] In the present case, however, we had to fit for B because the "house" logic suppressed only events that *followed* the μ^- in time, causing the $t<0$ background to exceed B.

Figure 5(a) displays in the form $N_{n/\gamma}(t)e^{+\Lambda_- t}$ the

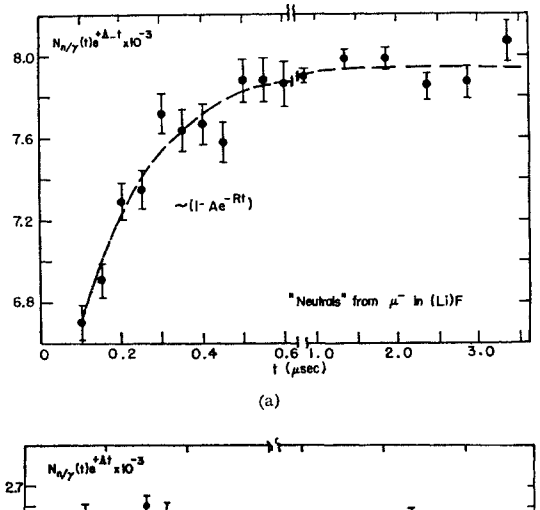

FIG. 5 (a). Time dependence of neutral capture products (neutrons and gammas), $N_{n/\gamma}(t)$, from (Li)F, corrected for background and asymptotic exponential dependence ($\Lambda_-=0.69$ μsec^{-1}). Dashed curve is best fit to data with $A=0.29\pm0.02$, $R=5.8\pm0.8$ μsec^{-1}. (b). Time dependence of neutral capture products (neutrons and gammas), $N_{n/\gamma}(t)$, from (Li)O(H), corrected for background and exponential dependence ($\Lambda=0.61$ μsec^{-1}). Dashed curve is the fitted mean. Note change in time scale for $t>0.6$ μsec.

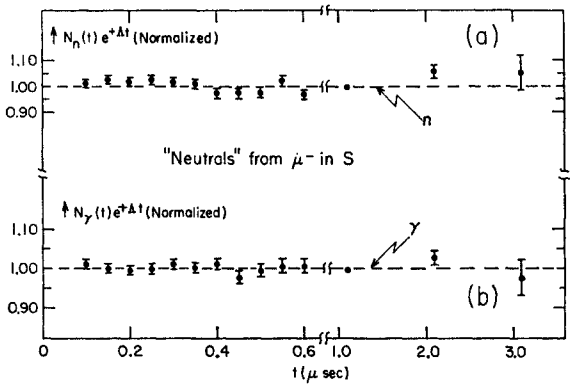

FIG. 6. (a). Time dependence of neutrons, $N_n(t)$, from S, corrected for background and exponential dependence ($\Lambda=1.79$ μsec^{-1}) and normalized to 1.00. Dashed curve is the fitted mean. (b). Time dependence of gammas, $N_\gamma(t)$, from S, corrected for background and exponential dependence ($\Lambda=1.80$ μsec^{-1}) and normalized to 1.00. Dashed curve is the fitted mean. Note change in time scale for $t>0.6$ μsec.

total $N_{n/\gamma}$ data (background subtracted). In the absence of any spin dependence, such a plot should yield, of course, a horizontal line. Instead, there is a striking dip at early times ($t<0.5$ μsec) exhibiting the spin-dependent effect sought.[59] To prove that this effect is not instrumental, we ran under identical conditions (i) a matched target of LiOH, in which effectively only O^{16} ($I=0$) captures, and (ii) a sulfur target ($I=0$). These control data were fitted to $f(t)=Ce^{-\Lambda t}+B$ for *all* t. As an additional check, we fitted the control data to $f(t)=C(1-Ae^{-Rt})e^{-\Lambda t}+B$ *assuming* the LiF value of R. Sufficiently good statistics were collected on S^{32} to analyze N_n and N_γ data separately, while only the $N_{n/\gamma}$ data of LiOH warranted analysis because the small $\Lambda^{\rm cap}(O^{16})$ limited the number of events obtained.

Figures 5(b) and 6 show that the control data are well fitted by pure exponentials.

Table III lists all information relevant to the fits. We note the following features: (a) The F^{19} capture rate, $\Lambda_-^{\rm cap}=(0.24\pm0.01)$ μsec^{-1}, agrees with measurements based on electron rates from[60] KHF_2 [$\Lambda^{\rm cap}=(0.254\pm0.022)$ μsec^{-1}] and[61] PbF_2 [$\Lambda^{\rm cap}=(0.24\pm0.04)$ μsec^{-1}]. The O^{16} and S^{32} capture rates also agree with electron measurements of reference 60. (b) The control data fits are consistent with $A\equiv0$.

F. Discussion of Results

The quantities of physical interest are the conversion rate R and $\Delta\Lambda/\bar{\Lambda}^{\rm cap}$, the latter being related to A by

$$\Delta\Lambda/\bar{\Lambda}^{\rm cap}=\frac{1}{n_+(0)}\frac{A}{1-A}$$
$$=\tfrac{4}{3}A/(1-A) \quad \text{for } F^{19} \quad (I=\tfrac{1}{2}). \quad (77)$$

[59] A preliminary 5-h run using a time converter [W. Weber, C. W. Johnstone, and L. Cranberg, Rev. Sci. Instr. 27, 166 (1956)]

TABLE III. "Neutrals data."

Run	Total events$\times 10^{-4}$	A	R (μsec^{-1})	Λ_- (μsec^{-1})	λ [a]	$(\chi^2-\langle\chi^2\rangle)/(2\langle\chi^2\rangle)^{1/2}$ [b]
LiF$-n$	7.1	0.36±0.04	6.2±1.0	0.69±0.01	50	0.18
LiF$-\gamma$	7.0	0.25±0.04	5.8±1.4	0.68±0.01	16	0.40
LiF$-n\gamma$	19.0	0.29±0.02	5.8±0.8	0.69±0.01	25	−0.70
LiOH$-n\gamma$	8.5	−0.01±0.03	···	0.61±0.01	12	−0.78
S$-n$	7.0	−0.04±0.025	···	1.79±0.01	180	1.6
S$-\gamma$	11.5	−0.02±0.02	···	1.80±0.01	70	−0.31

[a] λ = ratio of true to accidental background events at zero time.
[b] $\langle\chi^2\rangle$ = expected χ^2; $(2\langle\chi^2\rangle)^{1/2}$ ≈ standard deviation of χ^2 distribution.

Table VI compares the observed values with theoretical prediction. The values of R obtained from the various runs agree among themselves and are in excellent accord with theory. Note that the magnitude of $\Delta\Lambda/\bar{\Lambda}^{cap}$ derived from A_γ is less than that derived from A_n; while this discrepancy could (within statistics) be accounted for by a bremsstrahlung contamination of the $N_\gamma(t)$ measurement, it is not possible to rule out the branching ratio effects discussed in Sec. IV. A way out of this difficulty has been shown by Telegdi: With the occurence of conversion an experimentally established fact, the F^{19} capture rate measured for $t \gg R^{-1}$ (0.5 μsec, say) can be identified with $\Lambda_-^{cap}(F^{19})$. This can then be compared with $\bar{\Lambda}^{cap}(F^{19})$ obtained by interpolation on the Primakoff plot[11] to yield an independent estimate of $\Delta\Lambda/\bar{\Lambda}^{cap}$. This latter estimate yields $\Delta\Lambda/\bar{\Lambda}^{cap}=0.72$ ±0.09, i.e., agrees with the one derived from A_n. [A weakness in this argument lies in the fact that $\Lambda^{cap}(O^{16})$ as measured both in this experiment and by Sens,[60] lies about two standard deviations above the Primakoff plot.] This value of $\Delta\Lambda/\bar{\Lambda}^{cap}$ is in excellent agreement with the Primakoff[1] and Überall[9] predictions for a "universal $(V-xA)$" interaction ($x=1.21$). A $(V+xA)$ interaction is definitely ruled out by *either* the $N_n(t)$ of the $N_\gamma(t)$ measurement.

The values of the hyperfine parameters of F^{19} given by this experiment were corroborated by a measurement of the decay electron rate, $N_e(t)$ to be described in Sec. VII.

VI. F^{19} ELECTRON ASYMMETRY FOR $t \gg R^{-1}$

As an independent check of the "neutrals" evidence for rapid conversion in F^{19}, we compared the electron decay asymmetry parameter a of muons bound to F^{19} (UF_6 target) and C (graphite target) for $t>0.7$ μsec$\gg R^{-1}$. We used the precession method with a magnetic field of ≈110 G. As this measurement was carried out in conjunction with the "neutrals" experiment just described, the changes in the setup shown in Fig. 4(a) were minimal. They were: (a) the tank 9 was replaced by a 8-in.-square plastic scintillator 9′, placed flush against counter 8 to form the e^- telescope. The signature of an e^- was ($\bar{1}\,\bar{5}\,8\,9'$). (b) The "house" counters 6 and 7 were removed from the set-up and the "house" logic disconnected. (c) A pair of Helmholtz coils (24-in. diam) maintained a vertical field of ≈110 G on the target.

The UF_6 target (7 g/cm^2) consisted of a thin-wall brass container, 4 in. square$\times\frac{3}{4}$ in., into which UF_6 was condensed[62] and was positioned flush against counter 8.

In order to calibrate the geometry, the decay asymmetry from μ^+ in graphite, for which a good geometry value ($a=-0.229\pm0.008$)[63] is known, was measured. We obtained $a=-0.18\pm0.01$. The same measurement was made with the UF_6 target and gave $a=-0.18$ ±0.01, i.e., a similar result.

Runs with μ^-'s in UF_6 and graphite targets were performed under the same conditions. The first 0.7 μsec of the UF_6 time distribution were discarded. For $t>0.7$ μsec, there was no residual electron activity from muons bound to high-Z nuclei.

We recall that in the absence of conversion, one expects $a(F^{19})/a(C^{12})\approx\frac{1}{2}$ while our evidence for conversion requires that the fluorine asymmetry be zero for $t \gg R^{-1}$. Figure 7 shows the result of $|a(F^{19})|<0.003$. The relevant parameters appear in Table IV. We note the following points: (a) Making the geometry correc-

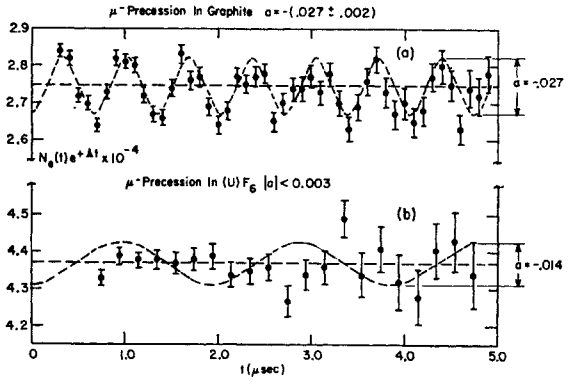

FIG. 7 (a). Precession of μ^- in graphite; $B\approx110$ G. (b). "Precession" of μ^- in UF_6, under conditions identical with those in (a). The exponential time dependence has been factored out for both (a) and (b) after subtracting background.

already demonstrated the presence of the early time dip in the $N_{n\gamma}$ time distribution.

[60] J. C. Sens, Phys. Rev. 113, 679 (1959).

[61] A. Astbury, I. M. Blair, M. Hussain, M. A. R. Kemp, and H. Muirhead (to be published).

[62] Thanks are due to N. M. Levitz of Argonne National Laboratory for providing us with the UF_6.

[63] R. A. Swanson, Phys. Rev. 112, 580 (1958).

TABLE IV. Precession data.

Run	Total events$\times 10^{-5}$	$a\times 10^2$	Λ_- (μsec^{-1})	λ [a]	$(\chi^2-\langle\chi^2\rangle)/(2\langle\chi^2\rangle)^{1/2}$ [b]
UF$_6$	3.2	0.27 ± 0.27	0.676 ± 0.006[c]	60	0.60
graphite	5.6	-2.7 ± 0.2	0.49[d]	480	0.80

[a] λ = ratio of true to accidental background events at zero time.
[b] $\langle\chi^2\rangle$ = expected χ^2; $(2\langle\chi^2\rangle)^{1/2}$ = standard deviation of χ^2 distribution.
[c] Corrected for C background; the error has been increased to include this source of uncertainty.
[d] Assumed from accepted value of C lifetime.

tion indicated by the calibration (i.e., 0.23/0.18) one gets $a(C^{12})=-0.035\pm0.003$ in fair agreement with the generally accepted value of -0.04. (b) The F^{19} disappearance rate obtained from electrons in $UF_6[\Lambda_-(F^{19})=(0.676\pm0.006)\ \mu\text{sec}^{-1}]$ is in fair agreement with $\Lambda_-(F^{19})=(0.69\pm0.01)\ \mu\text{sec}^{-1}$ measured in "neutrals."[64]

Our result is, for $t>0.7$ μsec, $|a(F^{19})/a(C^{12})|<0.1$, i.e., consistent with rapid conversion.

We remark that an entirely similar situation should obtain for P^{31}, where $R=58\ \mu\text{sec}^{-1}$ is predicted. There is conflicting experimental evidence on this point: A Dubna group reported $a(P^{31})/a(C^{12})\approx\frac{1}{2}$,[40] while experiments in Chicago show no asymmetry in P^{31}.[44]

VII. DECAY ELECTRON EXPERIMENT

The physical interest in a measurement of the hyperfine effect on the decay electron rate has already been discussed in Sec. III. In outline; (a) The hyperfine parameters measured in electrons are not subject to uncertainty from possible branching ratio effects. (b) One can determine at the same time the electron decay asymmetry in an $I>0$ nucleus. For these reasons, a measurement of $N_e^F(t)$ and $N_e^B(t)$ was performed on F^{19}.

A. Counting Setup

The experimental arrangement is shown in Fig. 8(a). The beam characteristics and method of identifying the muons have already been described. The only departure was a Čerenkov counter filled with FC-75 liquid ($n=1.28$) to anticoincidence the beam electrons. Without extra moderator ahead this counter was practically insensitive to muons.

The μ^-'s were brought into the setup through an aperature in a Pb wall sealed off by a large counter 1 as before. They traversed a beam-defining counter 2, Čerenkov counter 3, were moderated by copper (20 g/cm^2 total) passed through counters 4, 5, and 6 and stopped in a 12-g/cm^2 target, T, consisting of a single crystal of LiF ($3\frac{3}{4}\times3\frac{3}{4}\times2$ in.^{3}).[65] A number of Pb collimators, shown in the figure, physically defined the beam to ≈3 in. in diameter. Part of the Cu moderator (≈5 g/cm^2) was sandwiched between counters 5 and 6 for reasons given below. The stopped μ^-'s were identified by a $(12\bar{3}\,56\bar{7})$ coincidence. Counter 5 ($3\frac{1}{2}$-in.-diam disk) served to collimate the muons onto the target. Decay electrons from the target were detected in both forward and backward directions with respect to the incoming muon beam in separate telescopes; forward decays (e_F) were identified by a $(1\bar{6}78)$ coincidence, and backward decays (e_B) by a $(\bar{1}46)$ combination. The outputs of all three telescopes were fed to separate coincidence units of the type already described.[51] A longitudinal magnetic field of ≈100 G was maintained on the target by a pair of Helmholtz coils (24-in. diam) for the purpose of preventing precession of the μ^-'s about the cyclotron stray field and possible depolarization after coming to rest by local fields in the crystal.

The use of LiF for a fluorine target is not as well

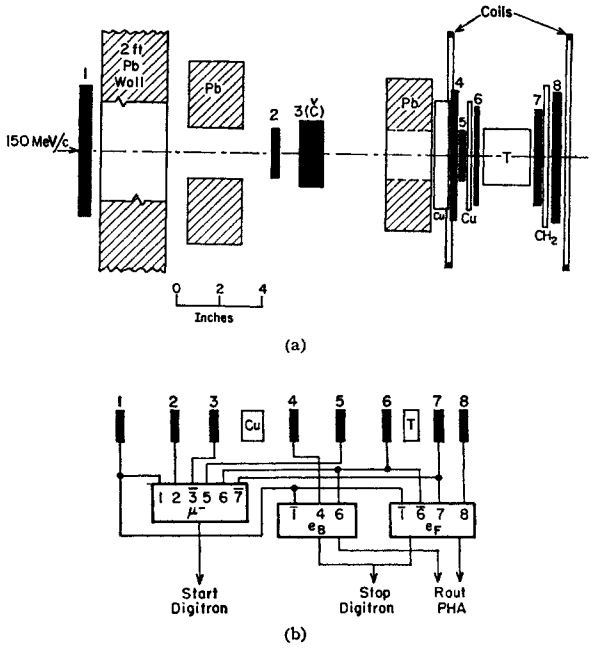

FIG. 8 (a). Experimental arrangement for decay electrons experiment. 1, 2, 4, 5, 6, 7, 8, plastic scintillators, viz., $1=8\times8\times\frac{1}{2}$ in.; $2=3\times3\times\frac{1}{4}$ in., $4=8\times8\times\frac{3}{8}$ in., $5=3\frac{1}{2}$-in. diam$\times\frac{3}{8}$ in., $6=6\times6\times\frac{1}{16}$ in., $7=6\times6\times\frac{1}{4}$ in., $8=8\times8\times\frac{3}{8}$ in.; 3, $4\times4\times1$ in. Čerenkov counter filled with FC 75 liquid ($n=1.28$); Cu, CH_2, moderator; Pb, collimators; T, LiF target. (b). Block diagram of decay electrons experiment. $(1\,2\,\bar{3}\,5\,6\,\bar{7})=$"muon" signature; $(\bar{1}\,\bar{6}\,7\,8)=e_F$, forward emitted electrons; $(\bar{1}\,4\,6)=e_B$, backward emitted electrons.

[64] This value is subject to uncertainty from carbon background. The amount of carbon present $\approx1.5\%$ at $t=0$ was estimated experimentally by the method described in reference 14 and the observed disappearance rate was corrected for it. We feel, however, that the "neutrals" value for Λ_- is more reliable as it is not subject to this source of error.

[65] Kindly loaned to us by the Harshaw Chemical Company, Cleveland, Ohio, through the courtesy of E. C. Stewart.

justified here as in the "neutrals" experiment. However, we know from mesonic x-ray evidence[66] that only $\lesssim 20\%$ of μ^- stopped in LiF form Li atoms. Inasmuch as $\exp[-\Lambda(\mathrm{Li})t]$ is slowly varying over $t\sim R^{-1}$, this Li contribution is not expected to seriously perturb the hf parameters for F^{19}. This will be justified quantitatively in the section on data analysis.

B. Measurement of $N_e^F(t)$ and $N_e^B(t)$

The counting logic is shown schematically in Fig. 8(b). A μ^--coincidence started the digitron. The outputs of the e_F and e_B circuits were fed as stop signals to digitron, individual routing pulses from the e_F and e_B circuits causing the events to be recorded in appropriate, distinct 200-channel subsections of the PHA memory. The rejection of multiple start and multiple stop events by the digitron logic[53] guaranteed that e_F and e_B events were sampled alternately and independently of each other. The digitron used in this experiment was operated at 45.16 Mc/sec but was otherwise essentially identical with the one employed in the "neutrals" measurement.

Runs on LiF were alternated with control runs on a 9-g/cm² graphite target; $N_e^F(t)$ and $N_e^B(t)$, were recorded simultaneously for each run. The subsections of the PHA to which the e_F and e_B events were routed were periodically interchanged to guard against systematics. Our typical μ^- stop rate was ≈ 600/sec at a duty factor ≈ 5; the collection efficiency of each electron telescope was $\approx 15\%$.

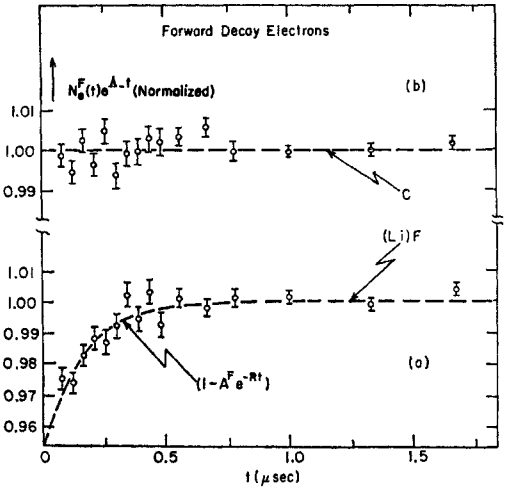

FIG. 9 (a). Time dependence of forward emitted electrons, $N_e^F(t)$, from (Li)F, corrected for background and asymptotic exponential dependence ($\Lambda_-=0.641$ $\mu\mathrm{sec}^{-1}$) and normalized to 1.00 for $t\gg 1/R$. Dashed curve is best fit to data with $A^F=0.048\pm 0.008$, $R=6.3\pm 1.8$ $\mu\mathrm{sec}^{-1}$. (b). Time dependence of forward emitted electrons, $N_e^F(t)$, from graphite, corrected for background and exponential dependence ($\Lambda=0.492$ $\mu\mathrm{sec}^{-1}$) and normalized to 1.00. Dashed curve is the fitted mean.

[66] J. F. Lathrop, R. A. Lundy, V. L. Telegdi, and R. Winston, Phys. Rev. Letters 7, 147 (1961).

C. Linearity and Backgrounds

The measurement of $N_e^B(t)$ was made difficult by spurious events near $t=0$ that tended to distort the time spectrum. These events could be attributed to the circumstance that the e_B telescope was traversed by the incident beam. Unwanted (46) coincidences not vetoed by a $\bar{1}$ signal could arise from: a coincidence with an afterpulse from counters 4 and 6 following the traversal of 4 and 6 by the incident muon; a π^- that stopped in 6 or T and produced a delayed event capable of triggering 4 and 6.

By employing selected phototubes in 4 and 6 and carefully shielding them against magnetic field, the afterpulsing was greatly reduced. Inserting ≈ 5 g/cm² of Cu between 4 and 6 suppressed the π^--induced events. A departure from linearity of $\lesssim 0.7\%$ for $t\geq 0.1$ μsec [as measured by the $N_e^B(t)$ spectrum of graphite] was finally achieved.

This experiment had two sources of background: decay electrons from stopped muons that did not form F atoms, and accidentals. The accidental background, as inferred from the $t<0$ time spectrum, was negligible ($\lambda>500$ in either e^- telescope). This low accidental background was due to digitron's multistart and multistop rejection. Our data analysis shows that $\approx(82\pm 4)\%$ of the stopped muons could be ascribed to F. Most of the remainder presumably formed Li atoms; the "carbon" contribution is estimated as $\lesssim 2\%$. For e_B events, ($\bar{1}46$), counter 6 is effectively a part of the target and contributes carbon background. For this reason, it was chosen thin (1/16 in.); no difference in the carbon components of $N_e^B(t)$ and $N_e^F(t)$ was found.

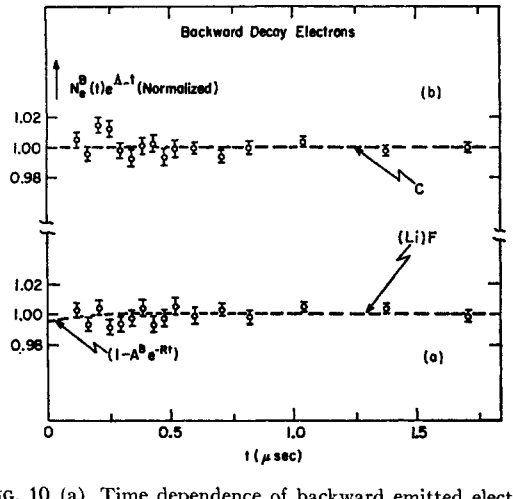

FIG. 10 (a). Time dependence of backward emitted electrons, $N_e^B(t)$, from (Li)F, corrected for background and asymptotic exponential dependence ($\Lambda_-=0.641$ $\mu\mathrm{sec}^{-1}$) and normalized to 1.00 for $t\gg 1/R$. Dashed curve is best fit to data with $A^B=0.0054\pm 0.011$, $R=6.3$ $\mu\mathrm{sec}^{-1}$. (b). Time dependence of backward emitted electrons, $N_e^B(t)$, from graphite, corrected for background and exponential dependence ($\Lambda=0.491$ $\mu\mathrm{sec}^{-1}$) and normalized to 1.00. Dashed curve is the fitted mean.

TABLE V. Decay electrons data.

Run	Total events$\times 10^{-6}$	$A\times 10^2$	R (μsec^{-1})	Λ_- (μsec^{-1})	λ [a]	$(\chi^2-\langle\chi^2\rangle)/(2\langle\chi^2\rangle)^{1/2}$ [b]
LiF e_F	2.2	4.7 $\pm$0.8	6.3$\pm$1.8	0.641$\pm$0.003	520	1.9
LiF e_B	1.1	0.54$\pm$1.1	...	0.641$\pm$0.004	980	0.20
C e_F	3.2	0.9 $\pm$0.6	...	0.492$\pm$0.002	560	1.9
C e_B	1.2	$-$0.1 $\pm$0.1	...	0.491$\pm$0.003	1000	2.1

[a] λ = ratio of true to accidental background events at zero time.
[b] $\langle\chi^2\rangle$ = expected χ^2; $(2\langle\chi^2\rangle)^{1/2}$ ≈ standard deviation of χ^2 distribution.

D. Data Analysis

The e_F data from the LiF runs were fitted to $f(t)=C(1-Ae^{-Rt})e^{-\Lambda_- t}+B$ for C, CA, R, and Λ_-. The (accidental) background term, B, was taken from the $t<0$ part of the data. The first three channels ($\approx$0.066 μsec) following $t=0$ were discarded for instrumental reasons (see Sec. V E). The e_F data from the graphite runs were treated in the same way, except that R was *assumed* to have the value given by the LiF e_F data. The fitted $f(t)$ was extrapolated to $t=0$ as described in Sec. V E. The treatment of the e_B data differed in only two respects: An additional two channels following $t=0$ were discarded for the reasons discussed in the preceding subsection. The value of R from the LiF e_F data was assumed for *both* LiF and graphite because the LiF e_B data were essentially a pure exponential and hence could not be used to infer R.

Figures 9(a) and 10(a) display in the form $N_e(t)e^{+\Lambda_- t}$ the background subtracted LiF e_F and e_B data, respectively. Figures 9(b) and 10(b) are the corresponding plots for graphite. Table V gives the results of the fits. We note that: The presence of a hyperfine effect ($A_e{}^F\neq 0$) in F^{19} is established to $\sim$6 standard deviations; R, as determined from $N_e{}^F(t)$, is in agreement with the value measured in neutrals; both LiF e_B and graphite data are consistent with $A\equiv 0$ (i.e., a pure exponential); $\Lambda_-(F^{19})$ as determined from either $N_e{}^F(t)$ or $N_e{}^B(t)$ [$\Lambda_-=(0.641\pm 0.003)$ μsec^{-1}] is $\approx$7% smaller than $\Lambda_-(F^{19})=(0.69\pm 0.01)$ μsec^{-1} measured in the "neutrals" experiment; $\Lambda(C^{12})=(0.0492\pm 0.002)$ μsec^{-1} and (0.0491 ± 0.003) μsec^{-1} from graphite e_F and e_B data, respectively, is in good agreement with existing carbon lifetime measurements.[14,67] We attribute the reduction in Λ_- observed from LiF electrons to activity from muons bound primarily to Li. To estimate the Li contribution, we fitted the LiF data with varying amounts of Li activity, and found that (18$\pm$4)% assumed Li stops bring the electron and "neutrals" Λ_- into agreement. The implication of this for the hyperfine parameters is considered below.

E. Discussion of Results

The quantities to be compared with theory are: R, $\Delta\Lambda=[R/n_+(0)](\frac{1}{2})[A_e{}^F+A_e{}^B]$, and $a=-(\frac{1}{2})[A_e{}^F-A_e{}^B]$. To facilitate comparison with the "neutrals" results it is preferable to use $\Delta\Lambda/\bar{\Lambda}^{cap}$, obtaining $\bar{\Lambda}^{cap}$ from Λ_- measured in "neutrals" and $\Delta\Lambda$ measured in electrons via the relation $\bar{\Lambda}^{cap}=\Lambda_-{}^{cap}/[1+n_+(0)\Delta\Lambda]$. Table VI lists these as derived from the LiF fits uncorrected for the presence of Li and compares them with prediction. The effect of an 18% Li contamination is to increase R by 20%, decrease $\Delta\Lambda/\bar{\Lambda}^{cap}$ by 3% and decrease a by 20%. These corrections are less than the statistical errors for each parameter, i.e., not significant for our data. We conclude that:

(1) The hyperfine effect in decay electrons from F^{19} yields the same capture parameters (within one standard deviation) as the neutron measurement. Hence, the latter was not grossly affected by branching ratio effects.

(2) The electron decay asymmetry $a(\frac{1}{2})$ in F^{19} agrees with the simple recoupling prediction of $a(\frac{1}{2})=\frac{1}{2}$ $a(0)\approx -0.02$. Therefore, the muon is not subject to appreciable hyperfine depolarization *during* its cascade to the K shell.

(3) μ^- in crystalline LiF in a longitudinal field of $\sim$100 G are not subject to appreciable depolarization in the mesonic K shell.

VIII. CONCLUSIONS

As stated at the outset, the purpose of a measurement of the hyperfine effect in muon capture is to learn the relative sign of the Gamow-Teller to Fermi coupling constants effective in muon capture, the one additional piece of information still needed to verify, from experiments on *complex nuclei*, the universality of the "$V-xA$" interaction. If the *magnitude* of the ratio of Gamow-Teller to Fermi coupling constants is fixed at the UFI value (corresponding to $|x|=1.21$ in e capture) then Table VI shows that $x=-1.21$ is experimentally excluded while $\Delta\Lambda/\bar{\Lambda}^{cap}$ observed from neutrons and decay electrons in LiF agree well with $x=+1.21$. The reasons for favoring the neutron over the smaller gamma value for $\Delta\Lambda/\bar{\Lambda}^{cap}$ have been discussed in Sec. V.

It is of interest to relax the assumption $|x|=1.21$ and see what limit can be put on the strength of the Fermi coupling constant effective in muon capture. To do this it is necessary to express the parameters (G_F, G_G, and G_P) in the equivalent nonrelativistic Hamiltonian (2) in terms of the "muon-dressed" coupling constants (g_V, g_A, and g_P) in the relativistic

[67] R. A. Reiter, T. A. Romanowski, R. B. Sutton, and B. G. Chidley, Phys. Rev. Letters 5, 22 (1960).

TABLE VI. Comparison of results with theory.

	Observed from				Predicted for	
	$N_n(t)$	$N_\gamma(t)$	$\bar{\Lambda}^{cap}$, Λ_-^{cap} [a]	$N_e^{F(B)}(t)$	$V-xA$	$V+xA$
$\Delta\Lambda/\bar{\Lambda}^{cap}$	0.75±0.13	0.45±0.10	0.72±0.09	1.07 ±0.44	0.76[b]	0.02[c]
R (μsec^{-1})	6.2 ±1.0	5.8 ±1.4	···	6.3 ±1.8	5.8[d]	
a	···	···	···	−0.021±0.007	−0.02[e]	

[a] Obtained from the observed Λ_-^{cap} and $\bar{\Lambda}^{cap}$ interpolated on the Primakoff plot; see Sec. V.
[b] The UFI prediction using either Primakoff's (Eq. 13) or Überall's shell-model estimate for ξ.
[c] Including weak magnetism terms; their omission leads to an even smaller predicted value.
[d] This value supersedes the one given in reference 15 since it replaces the estimate of Eq. (31) by a Hartree calculated $u_{2s}^2(0)$.
[e] Obtained from $a(\frac{1}{2})=\frac{1}{2}a(0)$ [Eq. (59)].

interaction.[1] The relations, given by Primakoff,[1] are

$$G_F=g_V(1+\nu/2m_p),$$
$$G_G=g_A-g_V(1+\mu_p-\mu_n)\nu/2m_p, \quad (78)$$
$$G_P=[g_P-g_A-g_V(1+\mu_p-\mu_n)]\nu/2m_p,$$

where $\nu\equiv|\mathbf{\nu}|$, $m_p\equiv$proton mass, and μ_p, μ_n are the proton, neutron anomalous magnetic moments introduced into the interaction by weak magnetism. It is convenient to define $y\equiv g_V/g_A$, the ratio of Fermi to Gamow-Teller coupling constants. The UFI prediction is $y=-0.804$[1]; Fig. 11 (lower half) shows the variation with y of $\Delta\Lambda/\bar{\Lambda}^{cap}$ for both H^1 [Eqs. (9) and (78)] and F^{19}. The proportionality constant between $\Delta\Lambda/\bar{\Lambda}^{cap}$ (9,19) and $\Delta\Lambda/\bar{\Lambda}^{cap}(1,1)$ is provided by either Primakoff's[18] or Überall's shell-model[20] estimate for ξ. Since once one departs from the UFI value of y it is not consistent to retain the weak magnetism terms,[68] the (dashed) curve omitting these terms is also indicated. The heavy portion of the solid curve corresponds to a reasonable ($\approx\pm6\%$) uncertainty in the UFI value of y,[69] i.e., the allowed range of y consistent with UFI.

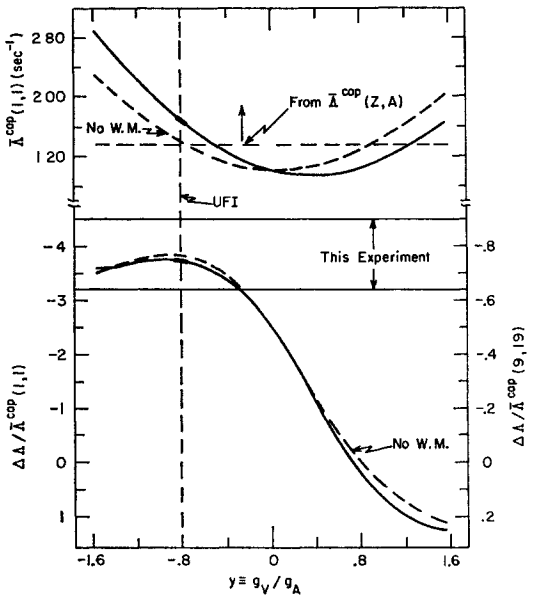

FIG. 11. (Lower half)—Plot of $\Delta\Lambda/\bar{\Lambda}^{cap}$ vs $y=g_V/g_A$ for H^1 (left ordinate) and F^{19} (right ordinate). The band indicated by this experiment represents the weighted mean of neutron and decay electrons results, viz., $\Delta\Lambda/\bar{\Lambda}^{cap}(9,19)=0.77\pm0.13$. (Upper half)—Plot of $\bar{\Lambda}^{cap}$ vs y for H^1. Horizontal dashed line corresponds to $\bar{\Lambda}^{cap}(1,1)\gtrsim135$ sec^{-1} derived from total capture rates of complex nuclei by the work of reference 5. Vertical dashed line indicates the UFI predicted value, $y=-0.804$. Heavy portions of solid curves correspond to $y=-0.804\pm0.05$. Dashed curves accompanying solid curves omit weak magnetism terms, i.e., the anomalous magnetic moments in Eq. (78).

The results of the measurements described in this paper that are relevant to muon capture are summarized by the weighted mean of the neutron and decay electron values for $\Delta\Lambda/\bar{\Lambda}^{cap}(9.19)$

$$\Delta\Lambda/\bar{\Lambda}^{cap}(9.19)=0.77\pm0.13. \quad (79a)$$

This gives with the ξ estimate mentioned above,

$$\Delta\Lambda/\bar{\Lambda}^{cap}(1,1)=3.9\pm0.7. \quad (79b)$$

In Eq. (79b) no allowance has been made for uncertainty in ξ. Note, however, that both ξ estimates coincide in the case of F^{19}.

Figure 11 shows that this result, while in excellent agreement with UFI ($y=-0.804$), is not very sensitive to the magnitude of y,[70] and, in fact, lies only about two standard deviations from $y\approx0$ (i.e., the absence of a Fermi coupling). We, therefore, appeal to the data on *total* capture rates of complex nuclei. Telegdi has shown[5] that the absence of a Fermi coupling is ruled out by a fit of the capture rates to Primakoff's closure formula[1,70a]:

$$\bar{\Lambda}(Z,A)/Z_{eff}^4=\gamma\bar{\Lambda}(1,1)[1-\delta(A-Z)/2A], \quad (80)$$

with

$$\gamma\equiv\langle\eta\rangle^2/0.58,$$

[68] I am indebted to Professor V. L. Telegdi for pointing this out to me.
[69] C. S. Wu, Rev. Mod. Phys. 31, 783 (1959).
[70] The insensitivity of this experiment to the presence of a Fermi coupling has been stressed by L. Wolfenstein, New York Meeting of the American Physical Society (1962).
[70a] *Note added in proof.* Since this paper was written, Klein and Wolfenstein [Phys. Rev. Letters 9, 408 (1962)] have raised doubts concerning the validity of Eq. (80). These authors argue that this formula is, even within Primakoff's closure approximation, *incomplete*, i.e., should be multiplied by a factor $(1-\Delta_a)$ where Δ_a is a parameter that depends on the nuclide "a" considered. The inclusion of this factor destroys the agreement with the UFI predictions, leading to a fitted value of $\bar{\Lambda}(1,1)$ twice as large as expected from universality. It is, however, to be noted that: (1) Fitting the Klein-Wolfenstein formula to the experimental capture rates for

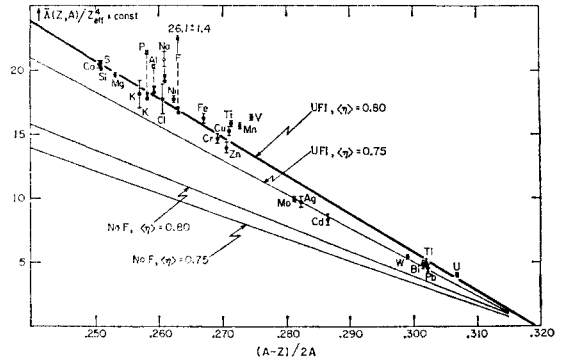

FIG. 12. (Reproduced from reference 5)—Experimental values of $\bar{\Lambda}(Z,A)/Z_{\text{eff}}^4$ vs $(A,Z)/2A$. Ordinate is actually $\pi a_0^3 \Lambda(Z,A)/Z_{\text{eff}}^4$ in units of 10^{-31} cm^3 sec^{-1}, as in reference 46. Heavy line through experimental points is best fit with $\delta=3.13$, $\gamma\bar{\Lambda}(1,1)=183$ sec^{-1}, i.e., corresponds to UFI with $\langle\eta\rangle=0.80$. Open circles represent experimental points not used in fit because they are affected by hyperfine effects; downward arrows represent estimated corrections (experimental for F^{19}, theoretical for others) for this spin dependence. All lines in the figure correspond to $\delta=3.13$, but to different assumptions about $\langle\eta\rangle$ and $\bar{\Lambda}(1,1)$, as indicated.

where we have used the notation of reference 5; the new parameter $\langle\eta\rangle$ depends on nuclear properties, the other terms have been defined in Sec. II.

Figure 12, which reproduces for convenience Fig. 1 of reference 5, illustrates the argument. Entirely similar reasoning puts a lower limit on the amount of Fermi coupling present; it is evident from Fig. 12, that $\gamma\bar{\Lambda}(1,1)$ should be at least as large as the value corresponding to the choice UFI, $\langle\eta\rangle=0.75$ in order that Eq. (80) give a reasonable fit to the observed capture rates. This implies, with $\langle\eta\rangle<0.84$ given by reference 5,

$$\bar{\Lambda}^{\text{cap}}(1,1)\gtrsim 135 \text{ sec}^{-1}. \tag{81}$$

Figure 11 shows that (81) taken together with the hyperfine result (79b) yields

$$y\lesssim -0.50 \tag{82a}$$

if weak magnetism terms are retained, or

$$y\lesssim -0.74 \tag{82b}$$

if weak magnetism terms are dropped.

Thus the two sets of data complement each other. The total capture rates yield a lower limit on the magnitude of $y\equiv g_V/g_A$ but cannot easily distinguish its sign; this the hyperfine data do decisively.[71]

ACKNOWLEDGMENTS

I wish to express my deep gratitude to Professor V. L. Telegdi for the patient instruction, guidance, and suggestions that have made this work possible and for his invaluable contributions in the preparation and performance of these experiments and in carrying out the theoretical work. The contributions of R. A. Lundy in the preparation and performance of these experiments were vital to their progress and I am greatly indebted to him. It is a pleasure to thank W. A. Cramer, G. Culligan, and J. F. Lathrop for their assistance in performing the experiments and D. Norman for technical aid with the equipment.

$20\leq Z\leq 92$, one obtains a 2.5 times larger χ^2-value than with Eq. (80); (2) agreement with UFI can be obtained, within the framework of the Klein-Wolfenstein formula, allowing a linear increase of δ with Z by only 20% over the Z range of interest. Both these points were raised by Professor Primakoff, to whom I am indebted for a stimulating discussion.

[71] As already emphasized in Sec. I, entirely similar conclusions have been reached from the observed μ-capture rate in liquid hydrogen (see references 2–4); thus reference 2 concluded that the capture rate is consistent with UFI and excludes a "$V+A$" interaction, while reference 3 assuming *only* experimental uncertainty, finds $y=-0.70\pm0.21$. We have attempted to show in this work that the universality of the "$V-xA$" interaction may be verified from experiments on *complex nuclei* alone.